LINEAR PHASE FIR LOW PASS DIGITAL DIFFERENTIATOR DESIGN

Thesis submitted in the partial fulfillment of requirement for the award of degree of

Master of Engineering

in

Electronics and Communication Engineering

Submitted by:

Simranjot Singh

Roll No 801061024

Under the guidance of:

Dr. Kulbir Singh

Associate Professor

ELECTRONICS AND COMMUNICATION ENGINEERING DEPARTMENT

THAPAR UNIVERSITY

(Established under the section 3 of UGC Act, 1956)

PATIALA – 147004 (PUNJAB)

DECLARATION

I, Simranjot Singh, hereby certify that the work which is being presented in this thesis entitled "LINEAR PHASE FIR LOW PASS DIGITAL DIFFERENTIATOR DESIGN" by me in partial fulfilment of the requirements for the award of degree of Master of Engineering in Electronics and Communication Engineering from Thapar University (Deemed University), Patiala, is an authentic record of my own work carried out under the supervision of **Dr. Kulbir Singh**.

The matter presented in this thesis has not been submitted in any other University / Institute for the award of any other degree.

Date: 11/06/12

Simranjot Singh
Roll No. 801061024

It is certified that the above statement made by the student is correct to the best of my knowledge and belief.

Date: 11/06/2012

Dr. Kulbir Singh
Associate Professor, ECED
Thapar University, Patiala

Countersigned by:

(Dr. Rajesh Khanna)
Professor and Head ECED
Thapar University, Patiala
Date:

(Dr. S.K. Mohapatra)
Dean of Academic Affairs
Thapar University, Patiala
Date:

ACKNOWLEDGEMENT

I would like to express my gratitude to **Dr. Kulbir Singh**, Associate Professor, Electronics and Communication Engineering Department, Thapar University, Patiala for his patience guidance and support throughout this thesis work. I am truly very fortunate to have the opportunity to work with him. He has provided me help in technical writing and presentation style, and I found this guidance to be extremely valuable.

I am very thankful to the Head of the Department, **Dr. Rajesh Khanna**, for his encouragement, support and providing the facilities for the completion of this thesis.

I am also thankful to entire faculty and staff members of Electronics and Communication Engineering Department for their unyielding encouragement.

I am greatly indebted to all my friends, who have graciously applied themselves to the task of helping me with ample morale support and valuable suggestions. Finally, I would like to extend my gratitude to all those persons who directly or indirectly helped me in process and contribute towards this work.

(Simranjot Singh)

ABSTRACT

Digital Differentiator is a vital signal processing tool. It is found in many applications, from low frequency biomedical equipment to high frequency radars. New developing fields such as touch screen tablets and online signature verification also has digital differentiators as basic building block. Many methods have been developed to design all types of differentiators but there is still scope of improvement in terms of parameters' optimization. The design problem of differentiators is a challenging task. Therefore, there is strong motivation to make design process easy and efficient.

First, the design of non-recursive linear phase higher order low pass digital differentiators, satisfying given specifications, is investigated. The concept of low pass differentiation is further generalized to higher order case. The design is based on Fourier series method for design of filters along with Kaiser Window function. The procedure is then used to design first order differentiators and results are compared with currently available techniques. The proposed FIR low pass differentiator has improvement in transition width and flexibility to choose any cutoff frequency. The same technique has been demonstrated for second order design according to provided specifications. This method is used to design second order low pass differentiator for QRS detection in ECG. It is shown that the proposed system has low hardware and software complexity as compared to existing second derivative based techniques of QRS detection.

Secondly, design of fractional order linear phase FIR digital differentiators is also investigated using convex optimization. Convex optimization has been applied to many engineering applications in recent years. This approach relies on finding optimum values of convex functions (e.g. linear phase FIR filters). It also requires less number of computations due to introduction of efficient algorithms. The problem of differentiator design is first described in terms of convex optimization with different optimization variables' options. The method is then used to design first order low pass differentiators and improvement in results is observed. The concept of low pass differentiation is further generalized to fractional order differentiators. Fractional order differentiators are designed by using minmax (Chebyshev) technique on mean square error. Design examples demonstrate easier design procedure than available fractional order differentiator design methodologies. The approach also has more flexibility in terms of specification constraints. Improvement over existing fractional order differentiators is proved using mean square

error parameter in passband. Finally, fractional order differentiators are designed and used for texture enhancement of images. The designed fractional order differentiators are applied on different colour images to demonstrate various desired levels of sharpening.

CONTENTS

List of Abbreviations

AFOD	Adjustable Fractional Order Differentiator
DFT	Discrete Fourier Transform
DHT	Discrete Hartley Transform
ECG	Electrocardiogram
FFT	Fast Fourier Transform
FIR	Finite Impulse Response
FOD	Fractional Order Differentiator
FOID	Fractional Order Integrator Differentiator
GL	Grunwald and Letnikov
HOD	Higher Order Differentiator
IDFT	Inverse Discrete Fourier Transform
IIR	Infinite Impulse Response
LPDD	Low Pass Digital Differentiator
LPF	Low Pass Filter
MMSE	Minimum Mean Square Error
MSE	Mean Square Error
RBF	Radial Basis Function
RL	Riemann and Liouville
RMS	Root Mean Square
WLS	Weighted Least Square

List of Figures

List of Tables

Chapter –1

Introduction

1.1 Digital Differentiators

Differentiation is an important signal processing tool [49]. There are many signal processing applications which require the determination or estimation of the time derivatives of a given signal. It gives a measure of instantaneous rate of change or slope. Typically, for example, in radars and sonars, the velocity and acceleration are computed from the position measurements using differentiation. Because output of a differentiator for exponential input can be found as [6]

$$\exp(j\omega t) \xrightarrow{D} j\omega \exp(j\omega t) \tag{1.1}$$

The corresponding impulse response for a differentiator is given by following equation. The impulse response of an eleven point differentiator is shown in Figure 1.1(a).

$$h[n] = \begin{cases} \dfrac{\cos(n\pi)}{nT}, & n \neq 0 \\ 0, & n = 0 \end{cases} \tag{1.2}$$

The frequency response of a differentiator is straight line passing through origin. So it is essentially a high pass filter. The impulse response is anti-symmetric. The magnitude response of a differentiator with eleven coefficients is shown in Figure 1.1(b).

In Figure 1.1(c) note the error is large around $\omega = \pi$ (for $\omega > .8\ \pi$). Clearly linearly increasing magnitude is not achieved over whole band and relative error is very high for low frequencies and high frequencies (around $\omega = \pi$).

1.2 Higher and Fractional Order Digital Differentiators

Differentiation and integration are usually regarded as discrete operations, in the sense that we differentiate or integrate a function once, twice, or any whole number of times. However, in some circumstances it's useful to evaluate a fractional derivative.

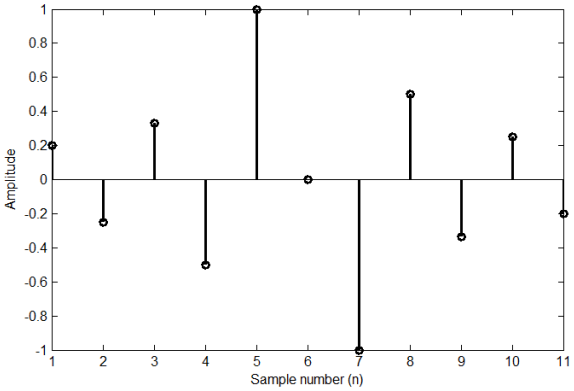

(a)

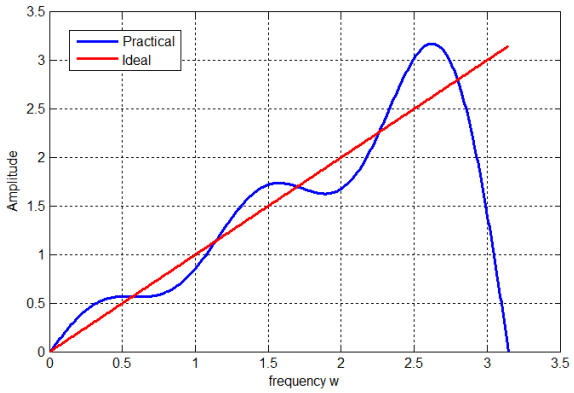

(b)

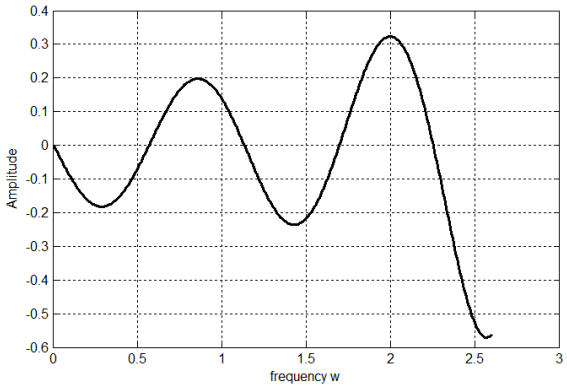

(c)

Figure 1.1: Digital Differentiator example (a) Impulse response of the differentiator (b) Magnitude response of the differentiator (c) Error in magnitude response of the differentiator

Fractional Calculus [27], [28] is generalization of ordinary differentiation and integration to non-integer order i.e. taking real number powers of differentiation operator

$$D^v f(x) = \frac{d^v f(x)}{dx^v}$$

If v is a natural number then the case is called higher order differentiation. Positive real number v corresponds to fractional order differentiation. The historical developments culminated in two calculi which are based on the work of Riemann and Liouville (RL) at the one side and on the work of Grunwald and Letnikov (GL) on the other. The classical form of fractional calculus is given by the Riemann–Liouville integral. It is given by

$${}_aD_t^{-\alpha} f(t) = {}_aI_t^{\alpha} f(t) = \frac{1}{\Gamma(\alpha)} \int_a^t (t-\tau)^{\alpha-1} f(\tau) d\tau$$

The corresponding derivative is calculated using Lagrange's rule for differential operators. Computing nth order derivative over the integral of order $n-\alpha$, the α order derivative is obtained. It is important to remark that n is the nearest integer bigger than α.

$${}_aD_t^{\alpha} f(t) = \frac{d^n}{dt^n}\ {}_aD_t^{-(n-\alpha)} f(t) = \frac{d^n}{dt^n}\ {}_aI_t^{(n-\alpha)} f(t)$$

These techniques have been used by various authors [17], [54] to design FODs. Frequency response of ideal higher/fractional order digital differentiator is

$$H_d\left(e^{j\omega}\right) = (j\omega)^v$$

1.3 Low Pass Digital Differentiators

In practice with noise effects taken into account a "good" differentiator should satisfy following frequency response condition for certain frequency regions [11].

$$H(\omega) = j\omega \tag{1.3}$$

(i) Depending upon the frequency region the differentiators are classified as

a) Full band differentiator $0 < \omega < \frac{\pi}{T}$

b) Wide band differentiator $0 < \omega < \frac{0.7\pi}{T}$

c) Narrow band differentiator for small values of ω

(ii) Another class of differentiators is low pass differentiators. Low pass differentiator frequency response is given by

$$H_{LP}(j\omega) = \begin{cases} j\omega & , \quad |\omega| \leq \omega_c \\ 0 & , \quad \omega_c \leq |\omega| \leq \pi \end{cases} \tag{1.4}$$

where ω_c is cut-off frequency.

One of the major complications in the design of a differentiator is that it amplifies the high frequency noise as described in [24]. This problem becomes more serious with the increase of filter bandwidth and/or the order of the derivatives. In many applications, differentiation is followed by low-pass filtering. Differentiation is used to extract information about rapid transients in the signal. Low-pass filters are used to reject noise frequencies higher than the cutoff frequencies of the signal. Low-pass filtering and differentiation can be implemented as a single low-pass differentiator filter or by using a low-pass filter and a differentiating filter in cascade.

1.4 Digital Differentiator Applications

- In radars and sonars, the velocity and acceleration are computed from the position measurements using differentiation. Velocity is estimated by first order differentiation and acceleration by second order.

- The rate of liquid flow in a tank (which may be part of a chemical plant) is estimated from the derivative of the measured liquid level.

- In biomedical investigations, it is often necessary to obtain the first and higher order derivatives of the biomedical data, especially at low frequency ranges. For example in QRS complex detection in ECG.

- For geo-physical data processing, derivatives of the observation samples are usually needed for midband frequencies of the spectrum. Maximally flat differentiators near half Nyquist frequency are useful for this operation.

- The derivatives at high frequencies are useful for solving the problems of image restoration and image texture enhancement (to detect various features, like an edge, for example, of an object in the picture).

- The use of derivatives of various signals in control engineering (in auto-follow, servomechanism, robotics, artificial eye etc.) is also well known.

- Fractional dimension is used to measure some real-world data such as coastline, clouds, dust in the air, and network of neurons in the body. The fractional dimension has been applied widely to pattern recognition and classification. Fractional Order Differentiators are used to exploit such real world issues. Fractional Order Differentiators are also used in bar code readers.

1.5 Convex Optimization

Convex optimization has attracted a lot of attention in engineering fields over the last few years. It provides reliable and efficient solution to many optimization problems. [22], [36] and [45] are an excellent resource for convex optimization related materials and its applications, most of the overview part is taken from them. Convex optimization consists of convex analysis, numerical computation and optimization theory as constituent fields. Convex optimization has found application in many engineering areas such as signal processing, communication, statistics, networks etc. Software tools (e.g. [25] and [36]) are available to find global optimum with a little programming effort. New areas are reported and opportunity to explore is present. Many engineering problems can be posed as (1.5).

$$\begin{aligned} &\text{minimize} \quad f_0(x) \\ &\text{subject to} \quad f_i(x) \leq 0 \quad i = 1,2,\dots\dots,m \\ &\qquad\qquad h_i(x) = 0 \quad i = 1,2,\dots\dots,p \end{aligned} \tag{1.5}$$

where $f_0(x), f_i(x)$ and $h_i(x)$ are equality and inequality cost constraints. x is a vector which need to be found for given specifications. If $f_i(x)$ are convex and $h_i(x)$ are affine then any local optimum is global optimum value. The problems can be efficiently solved by recently developed interior point algorithm [44]. Many non-convex problems could possibly be solved by using some peculiar techniques, for example change of variables. This approach is utilized in magnitude FIR filter design for signal processing applications [7].

1.5.1 Convex Sets

A function $f : \boldsymbol{R}^n \rightarrow \boldsymbol{R}^m$ is affine if it can be represented as linear operation such as

$$f(x) = Ax + b$$

If it is a matrix valued function, i.e. $f : \boldsymbol{R}^n \rightarrow \boldsymbol{R}^{p\times q}$ then it has the form

$$f(x) = A_0 + A_1x_1 + \ldots + A_nx_n$$

where $A_i \in \boldsymbol{R}^{p\times q}$.

A set $S \subseteq \boldsymbol{R}^n$ is affine if line passing through any two points in S lies in S. Therefore S contains the linear combination of any two points in S. It can be expressed as, if $x_1, x_2 \in S$ and $\theta \in \boldsymbol{R}$ then, $\theta x_1 + (1-\theta)x_2 \in S$.

A set $S \subseteq \boldsymbol{R}^n$ is convex if line segment joining any of its points in S lies in S. It can be expressed as if $x_1, x_2 \in S$ and $0 \leq \theta \leq 1$ then $\theta x_1 + (1-\theta)x_2 \in S$, i.e. a set is convex if every point in the set can be seen by every other point, along an unobstructed straight path between them, where unobstructed means lying in the set. An example of affine set is given in Figure 1.2. Convex and non-convex sets are demonstrated in Figure. 1.3.

1.5.2 Convex and Quasiconvex Functions

A function $f : \boldsymbol{R}^n \rightarrow \boldsymbol{R}$ is convex if its domain $dom\, f$ is convex and for all $x_1, x_2 \in dom\, f$, $0 \leq \theta \leq 1$

$$f(\theta x_1 + (1-\theta)x_2) \leq \theta f(x_1) + (1-\theta)f(x_2) \qquad (1.6)$$

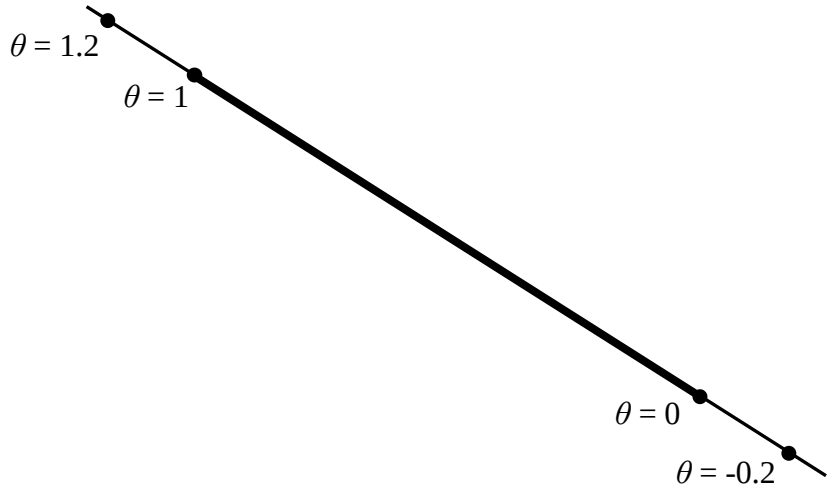

Figure 1.2: An example of affine set [45]

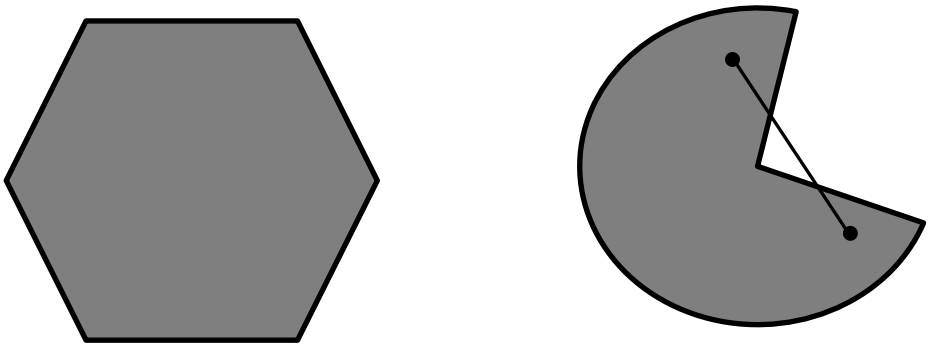

(a) (b)

Figure 1.3: Examples of Sets (a) Convex set example (b) Non convex set example

It is also known as Jensen's basic inequality. It can be extended to convex combinations of more points. So that if $x_1, x_2, \dots, x_k \in dom\, f$, $\theta_1, \theta_2, \dots, \theta_k \geq 0$ and $\theta_1 + \theta_2 + \dots + \theta_k = 1$ then

$$f(\theta_1 x_1 + \cdots + \theta_k x_k) \leq \theta_1 f(x_1) + \cdots + \theta_k f(k)$$

The continues case of Jensen's inequality : $p(x) \geq 0$ and $\int p(x)dx = 1$ then

$$f(\int xp(x)dx) \leq \int f(x)p(x)dx$$

$$f\big(\boldsymbol{E}(x)\big) \leq \boldsymbol{E}\big(f(x)\big) \tag{1.7}$$

f is concave if $-f$ is convex. Convex and non convex examples are illustrated in Figure 1.4. Some examples of convex function are x^2 for $dom\, \boldsymbol{R}$, $1/x$ for $dom\, \boldsymbol{R}_{++}$. Similarly $\log(x)$ is concave for $dom\, \boldsymbol{R}_{++}$. Affine functions such as $ax + b$ for $dom\, \boldsymbol{R}$ are examples of convex as well as concave functions.

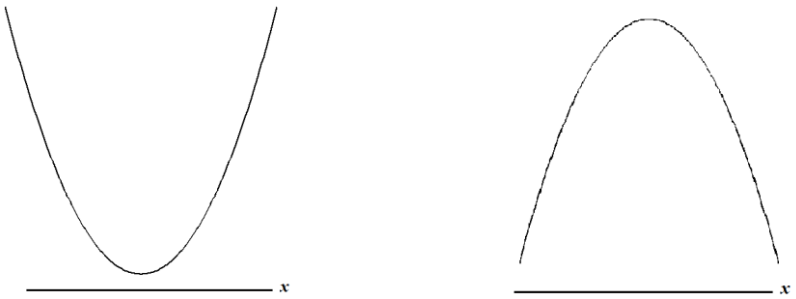

(a) (b)

Figure 1.4: Examples of functions (a) Convex function x^2 (b) Concave function $-x^2$

It is convenient to extend a convex function outside its domain. It is done by defining it ∞ outside dom. We can define extended value extension $\tilde{f}$ of a convex function f such that

$$\tilde{f}(x) = f(x) = \begin{cases} f(x), & x \in dom\, f \\ \infty, & x \notin dom\, f \end{cases} \tag{1.8}$$

This extension simplifies the notation as domain needs not to be provided explicitly every time a convex function is mentioned. Another important characteristic of functions is epigraph $epi\, f: \boldsymbol{R}^n \rightarrow \boldsymbol{R}$. Epigraph of a function f is defined as

$$epi\, f = \{(x,t)\} \mid x \in dom\, f, f(x) \leq t\} \tag{1.9}$$

Therefore if f is convex then $epi\, f$ is a convex set. It is a subset of $\boldsymbol{R}^{n+1}$ and means 'above the graph'. It is demonstrated in Figure 1.5.

The α sublevel set C_α of a function $f: \boldsymbol{R}^n \rightarrow \boldsymbol{R}$ is defined as

$$C_\alpha = \{\, x \in dom\, f \mid f(x) \leq \alpha\} \tag{1.10}$$

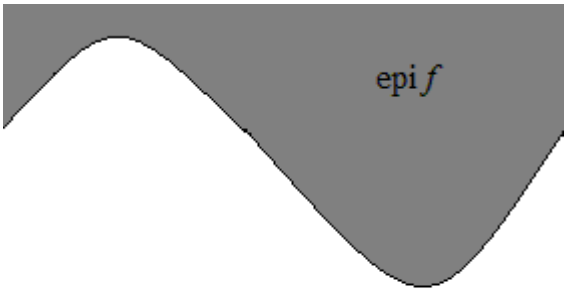

Figure 1.5: Epigraph of a function [45]

Sublevel sets of convex function are convex, however not vice versa. These properties are important in finding nature of the optimization problem in hand, as in the case of *quasiconvex* problems. Quasiconvex functions have locally flat regions. A function f is quasiconvex if its domain and all its subset levels are convex. If $-f$ is quasiconvex then f is quasiconcave. For example $\sqrt{|x|}$ is quasiconvex on $\boldsymbol{R}$.

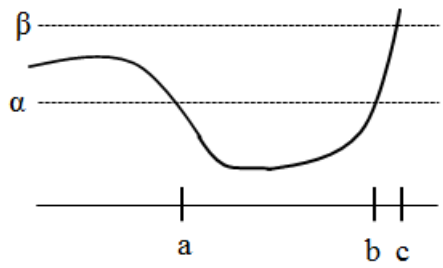

Figure 1.6: Different sublevel sets of a quasiconvex function [45]

The modified Jensen's inequality for quasiconvexity is

$$f(\theta x_1 + (1-\theta)x_2) \leq \max\{f(x_1) + f(x_2)\} \qquad (1.11)$$

Many engineering problems are quasiconvex in nature; however they can be solved by applying bisection optimization on the function.

Chapter 2

Literature Survey

In this chapter, overview of the work, regarding Digital Differentiators and their design methods, has been done.

2.1 Digital Differentiator Design

A procedure which can be used to design digital differentiators satisfying prescribed specifications was introduced by A. Antoniou [1]. The procedure is based on the Fourier-series method for the design of nonrecursive digital filters, and uses the Kaiser window function for the minimisation of the amplitude of Gibbs oscillations. The approach is used to design a number of differentiators assuming various prescribed bandwidths and various prescribed inband errors. It is also used to design a wideband high-precision differentiator. The proposed method is compared briefly with that of McClellan and Parks, based on the theory of weighted Chebyshev approximation.

A. Antoniou et al. [2] describes several improvements in the method reported by Antoniou [1] for the design of digital differentiators satisfying prescribed specifications. The improvements include the use of a more efficient optimisation algorithm, and a simple and accurate technique for the prediction of the required differentiator order. The improved design method is illustrated by several examples, and is compared with the equiripple design method.

L. R. Rabiner et al. [29] developed minimax relative error technique to design wideband differentiators using Remez optimization procedure. Observations made are such as the smaller the bandwidth, the faster the decrease of peak relative error with increasing order of differentiator (N). The larger the value of N, the faster the decrease of the peak relative error with decreasing bandwidth. Also it is established that differentiators with even values of N have peak relative errors which are approximately one to two orders of magnitude smaller than identical bandwidth differentiators with odd values of N.

Optimal, maximally accurate digital differentiators (DDS) are derived for the low-frequency range in B. Kumar et al. [8]. Exact coefficients used in the proposed DDs can

be readily computed from explicit formulas, whereas the optimal (minimal RE) DDs require and optimization program to derive the coefficients. The lower the frequency of differentiation, the better is the performance of the proposed differentiators, making them suitable for many typical applications

B. Kumar et al. [9] explored interrelationships between the digital differentiator (DD), the digital Hilbert transformer (DHT), and the half-band low-pass (1/2-LPF). A number of important properties confirming the close proximity of these filters has been highlighted. Theoretical results are produced by transforming minimax relative error DDs to equiripple DHTs and equiripple 1/2-LPFs. Relations connecting their impulse responses and their frequency responses are brought out. The precise frequencies of ripple extrema and the magnitudes of their peaks are shown to be simple related to the corresponding values for the minimax relative error differentiators.

Digital differentiators which are maximally linear at spot frequency $\omega = \pi/p$, where p is a positive integer, were proposed in B. Kumar et al. [10]. The suggested differentiator, besides giving zero phase error over entire set of frequencies, can achieve very high accuracy in the magnitude response over a given frequency.

M.A. Al-Alaoui [34] developed a novel class of stable, minimum phase, second-order, IIR digital differentiators. It is obtained by inverting the transfer functions of a class of second-order integrators, stabilizing the resulting transfer functions, and compensating their magnitudes. The responses of second-order integrators are obtained by interpolating the traditional Simpson and trapezoidal integrators. The resulting integrators have a perfect -90 degrees phase over the Nyquist interval and could better approximate the ideal magnitude response than either of the two traditional integrators. In addition to the above two integrators, the Tick integrator is also a member of the class. The resulting integrators and differentiators extend the frequency range of operation beyond that possible by using either of the two traditional integrators. The low order and high accuracy of the filters developed in this article make them attractive for real time applications.

A novel approach to designing recursive stable digital differentiators is discussed by M.A. Al-Alaoui [32]. A four step design procedure is presented. The procedure consists of obtaining or designing an integrator and then modifying its transfer function

approximately to obtain a stable differentiator. As an example a second order recursive differentiator is developed in this text.

A novel digital integrator and a novel digital differentiator were presented by M.A. Al-Alaoui [33]. Both the integrator and the differentiator are of first order and thus eminently suitable for real-time applications. Both have an almost linear phase. The integrator is obtained by interpolating two popular digital integration techniques, the rectangular and the trapezoidal rules. The resulting integrator outperforms both the rectangular and trapezoidal integrators in range and frequency. The new differentiator is obtained by taking the inverse of the transfer function of the integrator. The effective range of the differentiator is about 0.8 of the Nyquist frequency.

This work by M.A. Alaoui [35] addresses a direct approach to edge detection without using masks. In the process it describes two novel ideas, the direct approach and using IIR differentiators. Traditional edge detection relies on mask edge detectors based on FIR differentiators. The masks have to be small, thus the masks are based on low order FIR differentiators. It is well known that IIR digital filters outperform the same order FIR filters. Several differentiators are employed. The results show the superiority of the proposed approach.

A novel approach to the design of digital FIR differentiators is presented by C.C. Tseng et al. in [16]. The differentiator designed has linear phase and has zero derivatives at zero frequency. The design is based on the maximization of signal-to-noise ratio (SNR) at the output of the differentiator. The optimal filter coefficients have been obtained from the generalized eigenvector associated with the maximum eigenvalue of a pair of symmetric matrices. Estimation of the time derivative of polynomial signal, sinusoidal signal and handwritten Chinese signature is used to demonstrate that the proposed method provides better accuracy and higher SNR than the conventional differentiator method (eigenfilter).

In 2006, N.Q. Ngo [37] presented a general theory of the Newton–Cotes digital integrators and differentiators, which is derived by applying the z -transform technique to the closed-form Newton–Cotes integration formula. Based on this developed theory, a new wideband third-order trapezoidal digital integrator is found to be a class of trapezoidal digital integrators. Based on the designed wideband third-order trapezoidal

integrator, a new wideband digital differentiator is designed, which approximates the ideal differentiator reasonably well over the whole Nyquist frequency range and compares favorably with existing differentiators. The low orders and high accuracies of the novel wideband trapezoidal integrator and the new wideband differentiator has been proven attractive for real-time applications.

2.2 Low Pass Digital Differentiator Design

The design of Type III and Type IV linear-phase FIR lowpass digital differentiators according to the maximally flat criterion is described in I.W. Salesnick [24]. The author introduced a two-term recursive formula that enables the simple stable computation of the impulse response coefficients. The same recursive formula is valid for both Type III and Type IV solutions

A novel approach to design approximately linear phase infinite-impulse-response (IIR) digital filters in the passband region was introduced by M.A. Al-Alaoui [31]. The proposed approach yields digital IIR filters whose numerators represent linear phase finite-impulse-response (FIR) filters. As an example, low-pass IIR differentiators have been introduced in the paper. The range and high-frequency suppression of the proposed low-pass differentiators are comparable to those obtained by higher order FIR low-pass differentiators. In addition, the differentiators exhibit almost linear phases in the passband regions. These results are compared with Salesnick's [3] non recursive differentiators performance

2.3 Higher Order Design Differentiator Design

Eigenfilter technique was extended to design higher order FIR digital differentiators by S.C. Pei [47]. In this article filter coefficients are calculated by minimizing quadratic measure of error in frequency band. Filter coefficients are computed by finding an appropriate matrix's eigenvector. Described methodology is shown to be optimum in least square sense. Design examples are compared with Parks-McClellan algorithm. Eigenfilter approach has better performance in most of the frequency region except at cutoff frequency.

Optimal design of higher order digital differentiators in l_1 sense was studied by C.K. Chen et al. [18]. Conventionally, using l_1 error criterion for this design problem results in a nonlinear optimization problem since the corresponding objective function contains an absolute error function. The authors have first reformulated the design problem as a linear programming problem in frequency domain. To avoid the requirement of huge computation, an algorithm is proposed based on modification of Karmarkar's algorithm. This leads to very efficient procedure for the considered design problem. Simulations show better performance as compared to l_2 and Chebyshev error criteria.

G. Mollova et al. [20] proposes a new, simple analytic closed-form relation for least-squares design of higher-order differentiators. Using this approach, solving a system of linear equations for fullband differentiators is avoided. Numerical and graphical results are given in the paper for illustration.

The design method using eigenfilter approach is based on the computation of an eigenvector of an appropriate real, symmetric, and positive-definite matrix. The elements of this matrix are usually evaluated by very time-consuming numerical integration. S.C. Pei et al. [48] proposed a simple analytic closed-form formula to compute these matrix-elements very efficiently. Hence, the eigenfilter approach for differentiators becomes much easier and more accurate than before and design time is reduced greatly for designing long filters.

A new design technique for designing linear phase higher order differentiator was described by G.W. Medlin [21]. It is based on constrained quadratic optimization problem formulation. Their design method is based on a minimization procedure for integrated square error of the frequency response over designated frequency bands. The optimized design is formulated as a quadratic programming problem. The closed form solution is obtained by Langrange multipliers and is presented for the filter coefficients. Examples, for both even and odd length, that illustrate the design process are also given. The proposed technique has good error performance for low frequencies but relatively higher error levels at higher frequencies.

S.C. Pei et al. [46] proposed a fractional delay filter, an integer-order differintegrator, a fractional Hilbert transformer and a fractional differintegrator. Through the time-domain

analysis on the desired input and output signals of a linear time-invariant system, a set of linear equations are derived, which can be solved to obtain the coefficients of the desired filter. It is also showed that the difference between the desired output signal and the actual output of the system can be represented as the convolution of the derivative of the input signal and the Peano kernel. Design examples are illustrated to show the performance of each proposed filter. This method provides full band differentiator design whose performance for a given order is better than previous designs.

2.4 Fractional Order Digital Differentiator Design

A new method of the design of a fractional order FIR differentiator is invented by C.C. Tseng [12]. First, the fractional derivative of power function is defined. Then, the impulse response of fractional order differentiator is obtained by solving linear equations of Vandermonde form. Finally, one example is used to demonstrate that the fractional derivatives of digital signals are easily computed by using proposed filtering technique. This paper proposes easy recursive formulas to design fractional order differentiators with low error as compared to previous methods, differentiators of order 1, 1.5 and 2 are designed in one dimensional case.

The computation of a fractional derivative using the Fourier transform and a digital FIR differentiator is investigated by C.C. Tseng et al. [13]. First, the Cauchy integral formula is generalized to define the fractional derivative of functions. Then the fractional differentiation property of the Fourier transform of functions is presented. Using this property, the fractional derivative of a function can be computed in the frequency domain. A least-squares method to design the fractional order digital differentiator is designed next. When a signal passes through the designed differentiator, the output will be its fractional derivative. One design example is included to illustrate the effectiveness of this approach. Finally, the designed fractional order differentiator is used to generate a random fractal process which is better than the process obtained by the conventional method.

The design problems of variable fractional order integrator and differentiator (FOID) are investigated by C.C. Tseng et al. [14]. First, the transfer function of FOID is obtained by taking fractional power of the transfer function of conventional first order integrator and

differentiator. Then, to implement this irrational transfer function, the logarithm and Taylor series expansion are used to get a realizable approximated rational function. The proposed implementation structure is similar to the conventional Farrow structure of fractional sample delay filter. Next, the proposed approach is applied to design fractional rectangular integrator, fractional trapezoidal integrator, fractional Simpson integrator, fractional Al-Alaoui differentiator and fractional maximally flat differentiator. Finally, design examples are demonstrated to illustrate the performance of the proposed design method.

In C.C. Tseng et al. [15] the design and implementation structures of adjustable fractional order differentiator (AFOD) are discussed. First, the series expansion of ideal frequency response is used to transform the design of AFOD into the designs of log differentiators with various orders. Then, conventional FIR filter design method is applied to design log differentiators. The proposed method is flexible because the AFOD can be designed by considering the trade-off among the storage requirement of filter coefficients, implementation complexity and delay of filter. Finally, several numerical examples are shown to illustrate the effectiveness of the proposed design approach.

A discrete-time fractional-order differentiator being modelled as a finite-impulse response (FIR) system is explored by S. Samadi et al. [51]. The system yields fractional-order derivatives of Riemann-Liouville type for a uniformly sampled polynomial signal. The computation of the output signal is based on the additive combination of the weighted outputs of N cascaded first-order digital differentiators. For differentiators of fractional order with a terminal value equal to zero, the weights are time-varying. The weights are obtained in a closed form involving the Stirling numbers of the first kind. The system tends to a time-invariant integer-order differentiator when the order of the derivative tends to an integer value. It yields exact fractional- or integer-order derivatives of a sampled polynomial signal of a certain order

A new method for the design of fractional order differentiator was proposed by H. Zhao et al. [23]. Firstly, a fractional order differentiator (FOD) of power digital signal is defined in the frequency domain. Secondly, a FIR filter is chosen to approximate to the ideal digital FOD under the weighting mean square error (MMSE) sense of the frequency

response. Finally, design example and fractional derivative simulation are given and the advantages of the proposed method are illustrated.

The radial basis function based design of fractional order digital differentiator is investigated by C.C. Tseng et al. [17]. The radial basis function interpolation method is described. Then, the non-integer delay sample estimation of discrete-time sequence is derived by using the radial basis function interpolation approach. Next, the Grünwald–Letnikov derivative and non-integer delay sample estimation are applied to obtain the transfer function of fractional order digital differentiator. The fractional order digital differentiator designed has better approximation of ideal frequency response. The applications in digital image sharpening and parameter estimation of fractional noise process are studied to demonstrate the usefulness of this new design methodology.

Y.Q. Chen et al. [55] presented a new infinite impulse response (IIR) type digital fractional order differentiator (DFOD). This differentiator is proposed by using a new family of 2^{nd} order digital differentiators expressed in the second-order IIR filter form. The integer 2^{nd} order digital differentiators are obtained by the stable inversion of the weighted sum of Simpson integration rule and the trapezoidal integration rule. The distinguishing point of the proposed DFOD lies in an additional tuning knob to compromise the high-frequency approximation accuracy.

2.5 Gaps in the Study

Based on the literature review following gaps have been identified:

One dimensional fractional order differentiator design is studied in almost all articles. Thus, it would be interesting to extend the design methods to two dimensional fractional order differentiators.

The concept of low pass digital differentiation need to be extended to higher and fractional order case. Formula to design such filters is required to have a simple design method.

Convex optimization has not yet been utilized in design process of FODs. It would be interesting to compare convex optimization based FODs with existing FOD design techniques.

Low pass differentiators have not been employed in many applications. Similarly, applications of their higher order case may improve performance of present derivative based systems.

The design techniques of FODs encountered in literature, [17] and [23], require fairly complex programming and calculations.

Low pass differintegrator design can prove to be very useful in applications, such as with high frequency noise in system. Invention of their design algorithms is also an area that still needs to be explored. Optimization based methods may provide such options in differintegrator filters.

Linear phase FIR digital differentiators have been discussed throughout literature. However, improvement in terms of filter length, by using constraints on magnitude response, has not been done separately.

Analytic analysis of FODs is still a tedious task. Closed form formula for designing FODs will prove to be very useful in expanding field of fractional calculus applications.

2.6 Objective of Thesis

This thesis is having the following objectives:

(i) To generalize the concept of linear phase FIR low pass digital differentiators to higher and fractional order.
(ii) To design fractional order differentiator using convex optimization technique.
(iii) To design aforementioned differentiators with less computational effort, better flexibility and improved performance.
(iv) Application of these differentiators in QRS complex detection and image sharpening.

2.7 Organization of Thesis

This thesis consists of total six chapters which are organized as below:

Chapter 1: Introduction, it consists of introduction to various types of digital differentiators and their applications, a brief introduction to convex optimization is also provided in it.

Chapter 2: Literature Survey, vigorous study of research papers of related fields in sequence has been discussed.

Chapter 3: Digital Differentiator and FIR Filter Design, in this chapter current design methodologies of different types of differentiators, which are used in the report, are discussed in detail. Also, FIR filters and their design problem is briefly explored.

Chapter 4: Higher Order Low Pass Digital Differentiators, in this chapter higher order case of LPDD is investigated. Closed form expression is derived and used to design different examples. Application in the form of QRS complex detection in ECG signals is also described.

Chapter 5: Linear Phase FIR Fractional Order Digital Differentiators, in this chapter use of convex optimization to design fractional order digital differentiators is investigated. Low pass as well as full band options are formulated as convex optimization problem. Design examples are used in image texture enhancement of different images.

Chapter 6: Conclusion, in this chapter whole work has been concluded, on the basis of observations and also future scope has been discussed.

Chapter- 3

Digital Differentiator and FIR Filter Design

3.1 Introduction

Many Digital Differentiator design techniques have been introduced in recent years, as discussed in the literature survey. These methodologies aim to achieve minimum error in Nyquist interval of frequencies. In this chapter some of these methodologies have been explained, which have been very significant in this field. New design methods are required to be compared with these benchmarks to value their performance.

FIR filters are non-recursive filters having a transfer function of a polynomial in z and are an all-zero filter in the sense that the zeroes in the z -plane determine the frequency response magnitude characteristic. The z transform of an N -point FIR filter is given by

$$H(z) = \sum_{n=0}^{N-1} h(n) z^{-n} \tag{3.1}$$

It is described in detail in [19], [26], [50] and [53]. FIR filters are particularly useful for applications where exact linear phase response is required. The FIR filter is generally implemented in a non-recursive way which guarantees a stable filter. The FIR filters have a few advantages over the IIR filters [19]:

i. We can easily design the FIR filter to meet the required magnitude response in such a way that it achieves a constant group delay. *Group delay* is defined as $\tau = -(d\theta/d\omega)$, where θ is the phase response of the filter. The phase response of a filter with a constant group delay is therefore a linear function of frequency. It transmits all frequencies with the same amount of delay, which means that there will not be any phase distortion and the input signal will be delayed by a constant when it is transmitted to the output. A filter with a constant group delay is highly desirable in the transmission of digital signals.

ii. The FIR filters are always stable and are free from limit cycles that arise as a result of finite wordlength representation of multiplier constants and signal values.

iii. The effect of finite wordlength on the specified frequency response or the time-domain response or the output noise is smaller than that for IIR filters.

iv. Although the unit impulse response of an IIR filter is an infinitely long sequence, it is reasonable to assume in most practical cases that the value of the samples becomes almost negligible after a finite number; thus, choosing a sequence of finite length for the discrete-time signal allows us to use powerful numerical methods for processing signals of finite length.

3.2 Digital Differentiator Design

Digital Differentiators are required to satisfy maximally flat or maximally linear criteria i.e. they should have magnitude response of ideal differentiator in a band of frequencies. They can be low pass or band pass. The maximally flat FIR approximation to the ideal differentiator satisfies the derivative constraints given in [49] are

$$\left|H\left(e^{-j\omega}\right)\right| = 0$$

$$\frac{d\left|H\left(e^{-j\omega}\right)\right|}{d\omega} = 1$$

$$\frac{d^k\left|H\left(e^{-j\omega}\right)\right|}{d\omega^k} = 0 \qquad (3.2)$$

At frequency $\omega = 0$ and k ranging from 2 to B - 1, where B is the number of free parameters. Notice that the approximation is performed at a single frequency point $\omega = 0$. Kumar and Dutta Roy [49] described how the solution can be obtained from the maximally flat lowpass FIR filter.

3.2.1 Fourier Series Full Band Design Method

Antoniou [1] have used Fourier Series Method, as described in FIR Filter Design chapter, to design full band differentiators. His work to design the differentiators is given here. This method can be used to design full band and wide band differentiators. Nonrecursive digital differentiators can be designed by assuming an idealized periodic frequency response for the differentiator and then using the Fourier series to deduce the required

impulse response. The approach leads to an infinite-order nonrecursive digital filter and, hence, it becomes necessary to truncate the Fourier series.

The main difficulty with most of the window functions is that the amplitude of the residual oscillations is fixed once the order of the differentiator is fixed, and therefore the inherent design flexibility is limited. An alternative window function which overcomes this difficulty is one proposed by Kaiser. This window function involves an independent parameter α whose magnitude has a direct bearing on the amplitude of the residual for amplitude of Gibbs oscillations. The Fourier series is truncated by assigning (for N odd):

$$h(nT) = 0 \text{ for } |n| > (N-1)/2$$

Under these circumstances the amplitude response of differentiator is given by

$$M_D(\omega) = \left|H_D\left(e^{j\omega T}\right)\right| = H(z) = \sum_{n=-N_1}^{N_1} h(nT)e^{-j\omega T} \tag{3.3}$$

where $N_1 = (N-1)/2$

The amplitude response of the digital differentiator is given by

$$M_1(\omega) = |\omega| \text{ for } 0 \leq |\omega| < \omega_s/2$$

Error in amplitude response is the difference between desired and practical differentiator response

$$E(\omega) = M_D(\omega) - M_1(\omega)$$

Truncation of Fourier series causes error oscillations. Their amplitude is caused by slow convergence in Fourier series. The frequency of these oscillations increase with order N. The maximum of error oscillation remains virtually unchanged. However if Kaiser window is used for preconditioning of impulse response as given equation

$$h_w(nT) = w(nT)h(nT)$$

where $w(nT)$ is Kaiser window function and hence the amplitude response changes to

$$M_D(\omega) = \left|H_D e^{j\omega T}\right|$$

$$H_D(z) = \sum_n (w(nT)h(nT))z^{-n} \tag{3.4}$$

The Kaiser window is given in (3.5) using zeroth order Bessel function of first kind I_0. The effect of Kaiser window function on the amplitude response of the differentiator leads to a significant reduction in the amplitude of Gibbs oscillations.

$$w(n) = \frac{I_0(\alpha\sqrt{1-(n/N_1)^2})}{I_0(\alpha)} \; ; \; -N_1 \leq n \leq N_1 \tag{3.5}$$

Invariably, the digital differentiator is required to have a specific degree of accuracy over a specific range of frequencies, depending on the application and on the spectrum of $x(t)$. Hence, the prescribed specifications can be assumed to be the bandwidth of the differentiator and the corresponding inband accuracy. The bandwidth of a Kaiser differentiator can be defined to be the range of frequencies 0 to ω_p, for which

$$L(\alpha, N) \leq \delta$$

where $L(\alpha, N) = max|E(\omega)|$ for $0 \leq \omega \leq \omega_p$ and δ is prescribed.

For a given pair of values of N and ω_p, a well-defined optimum value of a exists for which $L(\alpha, N)$ is a global minimum.

The value of $L(\alpha, N)$ can be calculated by using following procedure:

i. Initialize α and N, say α =0.1 and N =3

ii. Minimize $L(\alpha, N)$ with respect to α until

$|L^k(\alpha, N) - L^{k-1}(\alpha, N)| \leq \varepsilon_1$ and $|\alpha^k - \alpha^{k-1}| \leq \varepsilon_2$

$L^k(\alpha, N)$ and α^k are the values of $L(\alpha, N)$ and α respectively at the end of k iteration minimization. $\varepsilon_1$and ε_2 are minimization tolerances.

iii. If $L^k(\alpha, N) \leq \delta$ then stop.

iv. Set $\alpha = \alpha^k$ and increment N by 2, continue to step 2.

Implementation of the Algorithm:

Minimization of $L(\alpha, N)$ with respect to α can be implemented using prescribed steps. The value of $L(\alpha, N)$ can be determined by using following procedure:

- Compute impulse response $h_w(nT)$ of the differentiator.
- Compute Error function $E(\omega)$ for frequencies in the range 0 to ω_p. A fine resolution of ω is necessary if an accurate estimate of $L(\alpha, N)$ is to be obtained. Fortunately maximum of $E(\omega)$ occurs near passband edge frequencies. As a result $E(\omega)$ need only to be evaluated over small range of frequencies, say from $m\omega_p$ to ω_p, where m is a fractional value depending upon N. If N is in between 10 to 30 then m = 0.8 is found to yield satisfactory results.
- Compute $L(\alpha, N)$ from maximum error in passband.

Prescribed value of inband accuracy should be satisfied while keeping N minimum. Therefore finding α again and again and increasing N, unless specifications are fulfilled.

Figure 3.1 illustrates the effect of using direct truncation(rectangular window) and utilizing Kaiser window. It is clearly seen that error amplitudes are reduced in Kaiser window case of the differentiator's magnitude response. The oscillations observed, known as Gibbs oscillations, are owing to the truncation of the Fourier series. Their large amplitude is caused by slow convergence in the Fourier series. As it can be seen, the frequency of these oscillations tends to increaseas N is increased. Maximum of these oscillations however remains unchanged.

Maximum error in passband, $L(\alpha, N)$, varies with passband cutoff frequency(ω_p). It is shown in Figure 3.2 and Figure 3.3, $L(\alpha, N)$ for different values of α and N are plotted for 1.5 π and 2.5 π taken as passband cutoff frequencies.

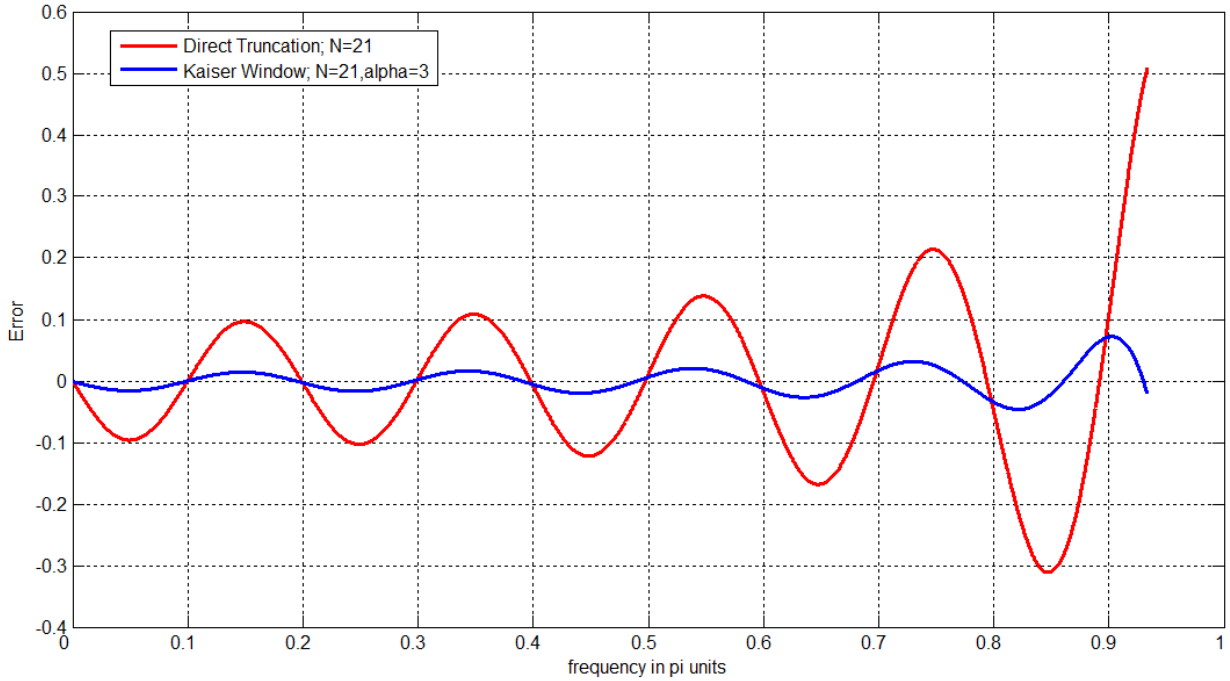

Figure 3.1: Error oscillations in filter's frequency response from direct truncation and Kaiser window truncation

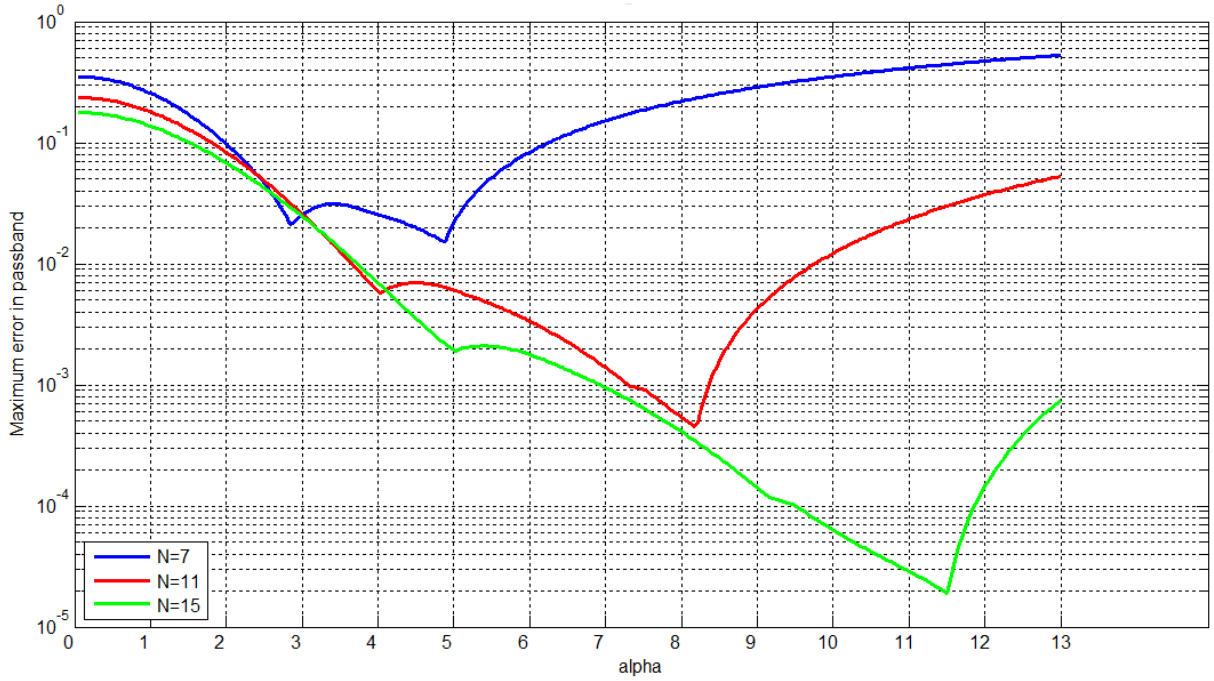

Figure 3.2: L curve for different filter orders and 1.5 π along α

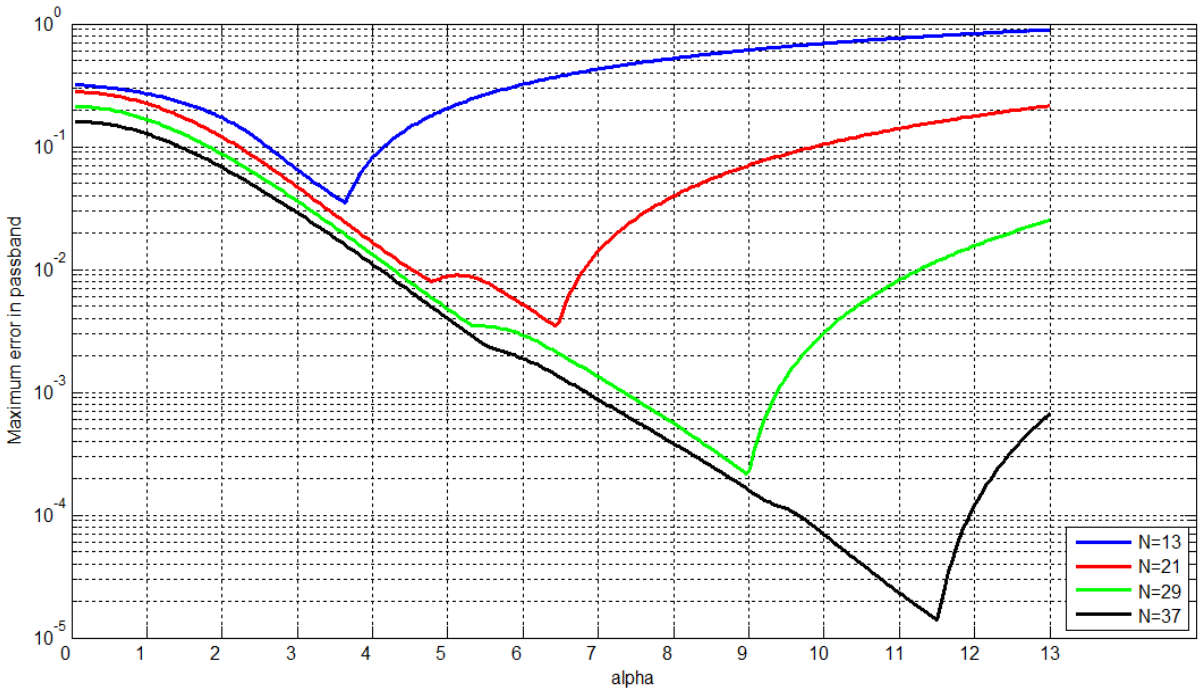

Figure 3.3: L curve for different filter orders and 2.5 π along α

The larger the value of passband frequency, more number of filter coefficients are required to achieve specific minimum error. As can be seen by comparing Figure 3.2 and Figure 3.3, optimum value of α depends on order of the filter.

The length of differentiator required to achieve minimum error comparable to 1.5 π passband, order of differentiator has to increase exponentially.

Design Example 1: This procedure was used to design three digital differentiators assuming a prescribed bandwidth ω_p = 2 rad/s and prescribed maximum inband errors δ = 0.01, 0.005 and 0.001. The variation of error (E) in passband with frequency is illustrated in Figure 3.4

Design Example 2: Again three digital differentiators are designed assuming a prescribed maximum inband error δ = 0.01 and prescribed bandwidths ω_p = 2.25, 2.5 and 2.75 rad/s. The variation of E with frequency is illustrated in Figure 3.5.

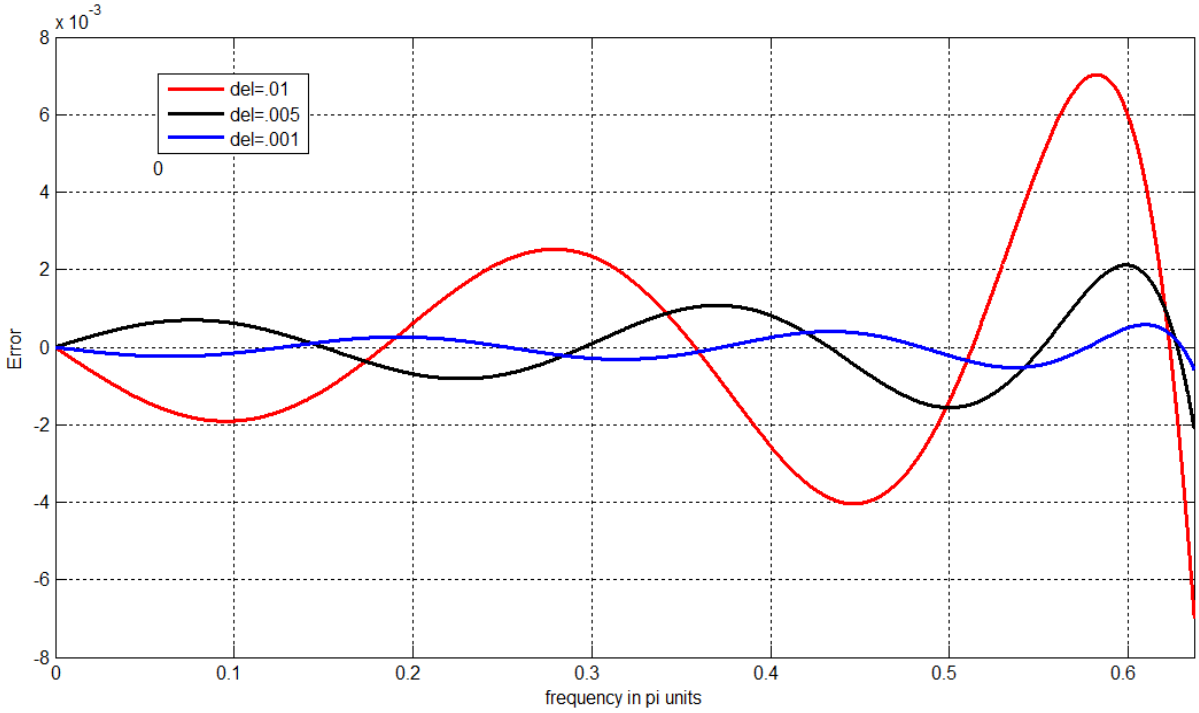

Figure 3.4: Error Plot: Design Example 1

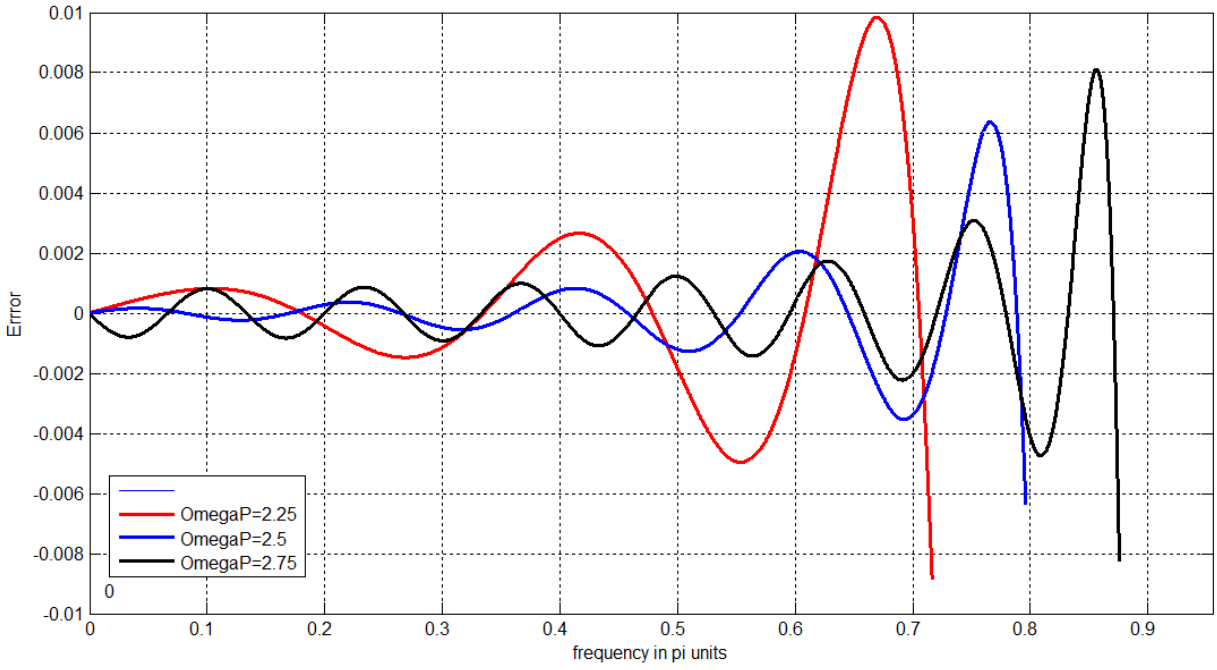

Figure 3.5. Error Plot: Design Example 2

Design Example 3: Finally, the procedure was used to design a wideband differentiator having a prescribed bandwidth of ω_p = 3.0 rad/s, and a prescribed maximum inband error δ =0.01. The optimum values of α and N were found to be α = 5.332918 , N = 77.

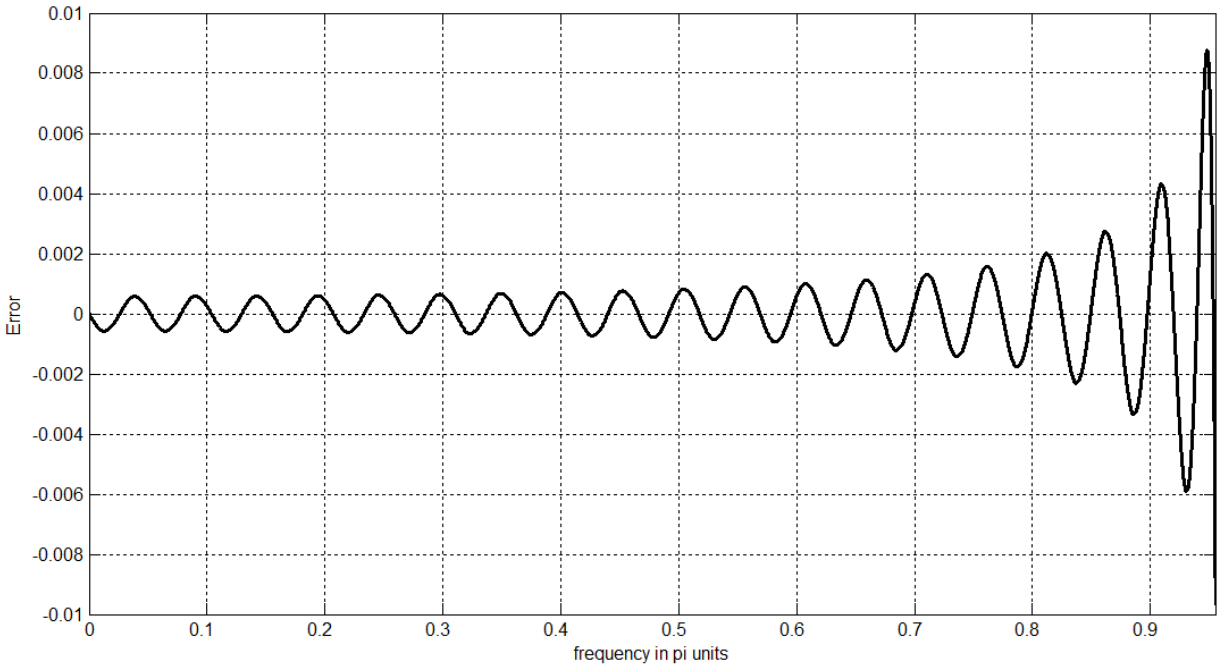

Figure 3.6: Error plot of a wideband differentiator designed using Fourier Series Method.

3.2.2 Low Pass Digital Differentiator Design

To avoid the undesirable amplification of noise in digital differentiation, lowpass differentiators can be used in place of full-band ones. They find application, for example, in bar code readers. A novel method to design low pass differentiators was introduced by [24]. Its extension to recursive case is done in [31]. The designing technique also provides a filter with linear phase.

3.2.2.1 Salesnick's Low Pass Differentiator

This method [24] describes the design of type III and type IV linear-phase finite-impulse response (FIR) low-pass digital differentiators according to the maximally flat criterion. A two-term recursive formula that enables the simple stable computation of the impulse response coefficients was introduced by Salesnick. The same recursive formula is valid for both Type III and Type IV solution. The derivation of the solution will depend on a transformation that maps polynomials on the real interval [0, 1] to polynomials on the upper half of the unit circle. Let K denote the number of zeros a transfer function has at $z = -1$. A Type III transfer function always has an odd number of zeros at $z = -1$. In terms of

K, we have K = 2 M +1 for Type III transfer function and K = 2 M for Type IV transfer function.

The transfer function of maximally flat linear phase low pass digital differentiator is given by

$$H(z) = \left(\frac{1 - z^{-1}}{2}\right)\left(\frac{1 - z^{-1}}{2}\right)^{K} z^{-L} \sum_{n=0}^{L} c(n) \left(\frac{-z + 2 - z^{-1}}{4}\right)^{n}$$

$$c(n) = \frac{(8n^2 + 4Kn - 10n - K + 3)c(n-1) - (2n + K - 3)^2 c(n-2)}{2n(2n+1)}$$

Magnitude response of maximally flat low pass differentiators designed using the Salesnick's method is given in Figure 3.7(a). It shows the frequency response for a family of Type III lowpass differentiators of length N = 29, where K is varied from 1 to 24 in increments of 4, and where L = (N − K)/2 - 1. Where K is number of zeros present at z = -1. As it can be seen as K is increased from 1 to 24 with keeping length of filter 29, the differentiator turns from full band to narrow band low pass differentiator. It would be interesting to find any other way to design low pass differentiator of same order with better transition characteristics. So by using recursive equations given by Salesnick Low pass differentiator with variable passband can be designed. Figure 3.7(b) illustrates error plot of the filter, error is in under 2% for the passband but the filter does not show sharp transitions.

3.2.2.2 Alaoui's Recursive Low Pass differentiator [31]:

The basic concept is to obtain an IIR filter that satisfies the magnitude specifications and exhibits a linear phase in the passband region. This could be realized by designing an IIR filter whose transfer function numerator polynomial represents a linear phase FIR filter and whose transfer function denominator polynomial contributes poles that provides the desired steep roll-off for the magnitude of the frequency response while preserving the linear phase in the passband region. The above is possible if the resulting function had poles and zeros that are sufficiently far apart.

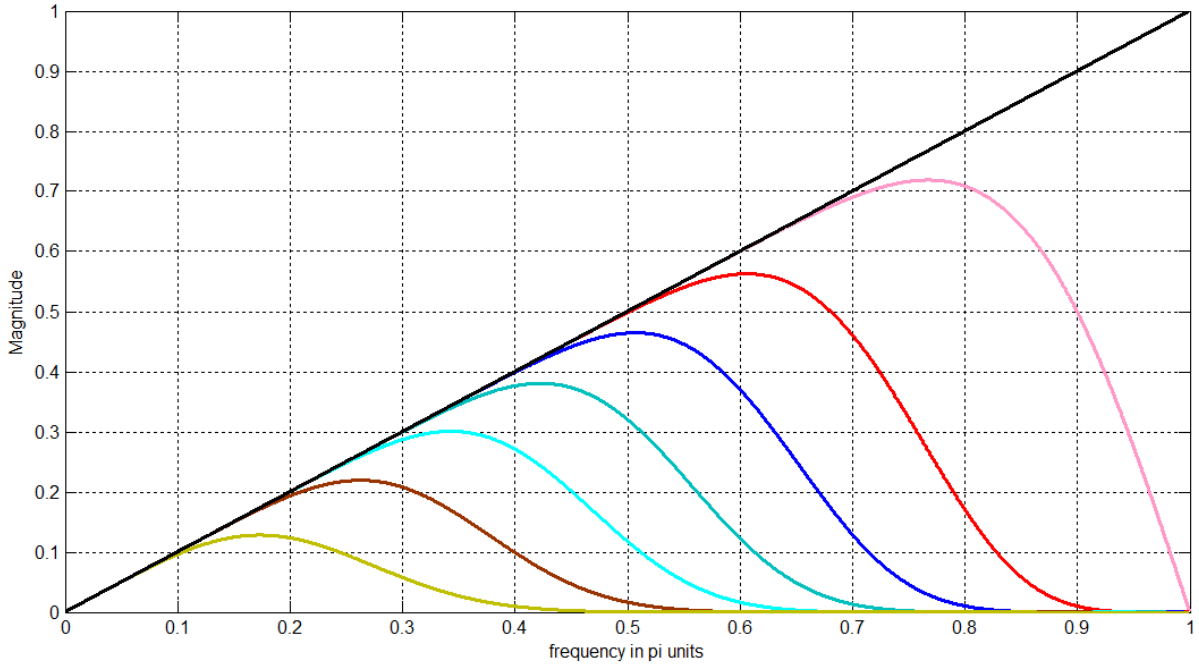

(a)

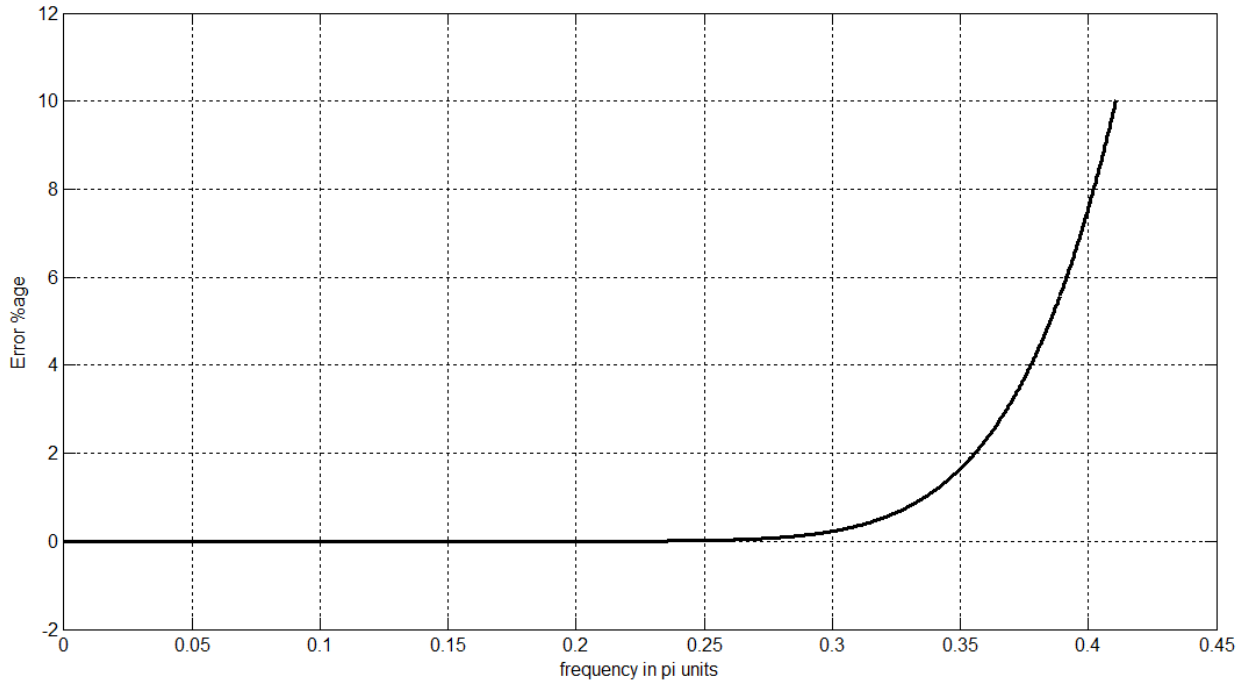

(b)

Figure 3.7: Salesnick Low pass differentiator for K=1:4:25 ; N=29 (a) Magnitude response (b) Error Plot

This proposed approach by Alaoui utilizes the linear phase properties of the FIR filters and the smaller transition band and the steeper roll-off properties of the IIR filters, compared to the same order FIR filter, to obtain low-order low-pass differentiators with an approximately linear phase in the passband region. The resulting IIR filter order should approximate a corresponding FIR filter with a greater order of reduction than had been obtained so far by other methods. The lowest ratio that was reported of the orders of the IIR filters, with linear phases in the passband, to the order of the FIR filters that they were approximating, was one fifth.

Two IIR differentiators are used in the construction of the low-pass differentiators. These are followed by two corresponding low pass filters. For brevity only third type low pass differentiator is discussed here.

Differentiator *:* This is a first-order, wide-band differentiator, obtained by interpolating the trapezoidal and the rectangular integration rules [32]–[34], and it is also known as the Al-Alaoui operator. The transfer function of this differentiator is given as follows:

$$H(z) = 0.3638\frac{(1 - z^{-1})}{(1 - \frac{z^{-1}}{7})} \tag{3.6}$$

It is to be noted that the numerator of (3.6) represents a length-2 odd symmetric FIR filter. It is also interesting to note that the numerator of (3.6) is the same, except for a gain factor.

Low pass filter : The differentiator I was cascaded with third order Chebyshev I low-pass filters having 0.1 dB ripple in the passband and obtained by using the bilinear transform. The numerator polynomial of the resulting transfer function, up to a multiplying constant, is as follows:

$$(1 - z^{-1})(1 - z^{-1})^3 = 1 + 2z^{-1} + 0z^{-2} - 2z^{-3} - z^{-4} \tag{3.7}$$

Equation (3.7) represents an antisymmetric with an odd length, type III, linear phase FIR filter. The coefficients of the resulting low-pass differentiators are ordered in descending powers of z to get a's and b's coefficients of the low pass filter. So the numerators will be antisymmetric to obtain linear phase as close to FIR counterparts. So that this

differentiator magnitudes exhibit shorter transition regions and thus better suppression of high-frequency noise compared with the state-of-the-art FIR filters.

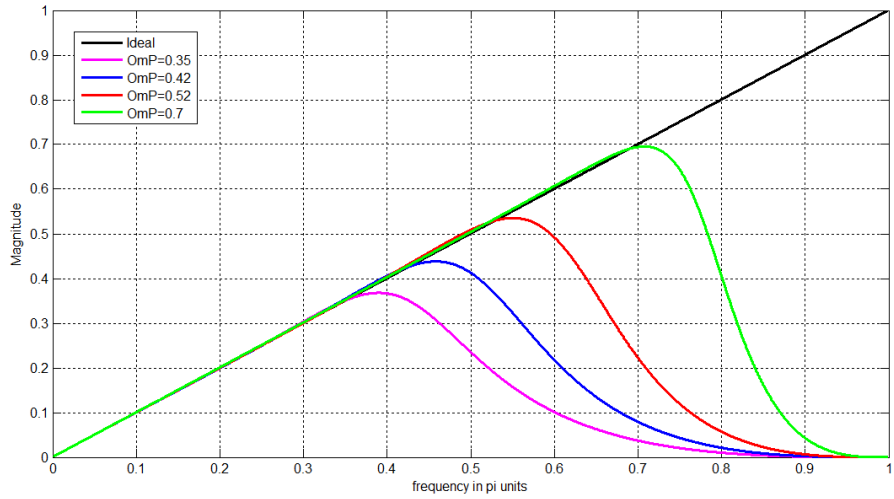

(a)

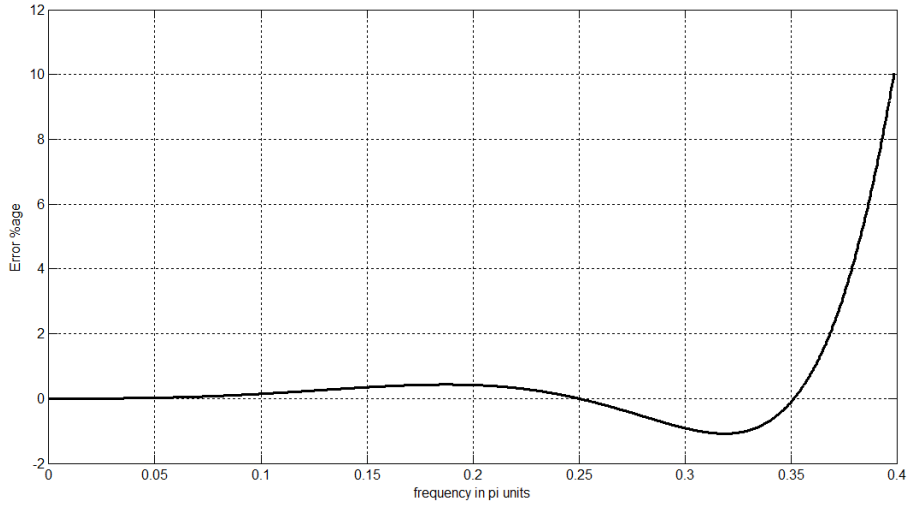

(b)

Figure 3.8: Al-Alaoui's method for LPDD design (a) Magnitude response of the differentiator for different ω (b) Error Plot

Digital Differentiator designed with Alaoui's method is shown in Figure 3.8(a). When compared with Salesnick's method, it surely show some improvement in less transition width. However,if we compare Figure 3.8(b) the percentage error of the proposed low-pass differentiator with a normalized cutoff frequency of 0.35 with that the FIR

differentiator of Selesnick. While the FIR low-pass filters outperform the proposed differentiator, the 2% error is acceptable in many applications.

3.2.3 Fractional Order Differentiator (FOD) design:

Fractional Calculus has attracted a lot of attention lately [27], [28] as discussed in chapter 1. So, FOD design techniques have been studied and researched in recent years. Some of the recently developed methods are explored here.

3.2.3.1 FOD design using Frequency Response Approximation [23]:

Zhao et al. introduced this method based on weighted mean square error approximation of frequency response. The principle behind this method is such that FIR filter is chosen to approximate to the ideal FOD under the weighting mean square error (MSE) sense of the frequency response. The steps to design a FOD with length 2 M and order q are:

(i) Compute T_a, T_b, I_a and I_b .

$$T_a(n,m) = \frac{1}{R}\int_{-\pi}^{\pi} W(\omega)\cos(m\omega)\cos(n\omega)\,d\omega + K$$

$$I_a(n) = \frac{1}{R}\cos\left(\frac{q\pi}{2}\right)\int_{-\pi}^{\pi} W(\omega)\,\omega^q\cos(n\omega)\,d\omega$$

$$T_b(n,m) = \frac{1}{R}\int_{-\pi}^{\pi} W(\omega)\sin(m\omega)\sin(n\omega)\,d\omega$$

$$I_a(n) = \frac{1}{R}\sin\left(\frac{q\pi}{2}\right)\int_{-\pi}^{\pi} W(\omega)\,sgn(\omega)\omega^q\sin(n\omega)\,d\omega \qquad (3.8)$$

(ii) Calculate $a(m)$ and $b(m)$ coefficients by using following equations:

$$\sum_{m=0}^{M} T_a(n,m)a(m) = I_a \qquad n = 0,1,\dots,M$$

$$\sum_{m=1}^{M} T_b(n,m)b(m) = I_b \qquad n = 1, \dots, M \tag{3.9}$$

where $R = \int_{-\pi}^{\pi} W(\omega)\, d\omega$ and K is offset.

(iii) Then $a(m)$ and $b(m)$ coefficients are used to obtain filter impulse response using following equation:

$$y(n-M) = a(0)x(n-M) + \sum_{m=1}^{M} \frac{a(m)+b(m)}{2} x(n-M+m) + \sum_{m=1}^{M} \frac{a(m)-b(m)}{2} x(n-M+m)$$

A design example [23] to design FOD with following q = 1.5, M = 5 and K = 1. Weighting function is taken as

$$W(\omega) = \begin{cases} 1, & \omega \le 0.72\,\pi \\ 0, & 0.72\,\pi \le \omega < \pi \end{cases}$$

Therefore, here the differentiator is designed by minimizing error up to 0.72 π

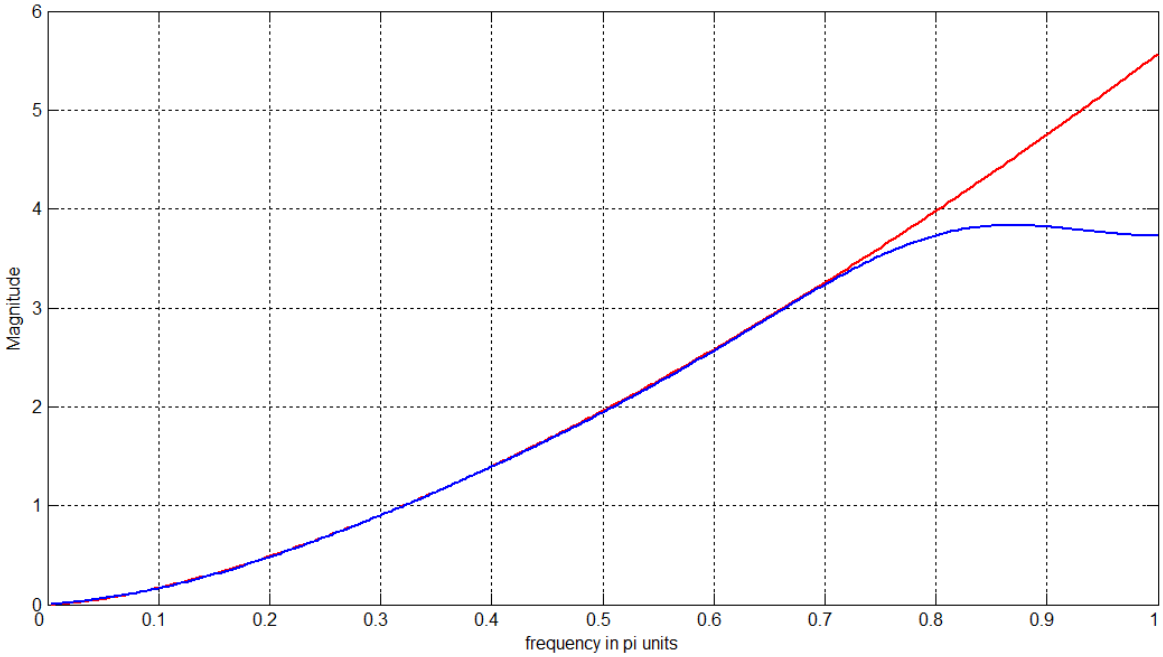

Figure 3.9: Magnitude response of designed FOD with q = 1.5 using [23]

3.2.3.2 FOD design using Radial Function Basis (RBF) [17]:

In 2010, Tseng et al. used RBF to design an FOD. A radial basis function is a real valued function whose value depends only on distance from the origin i.e. $\varphi(t) = \varphi(|t|)$. Commonly used RBF is Gaussian given by

$$\varphi(t) = e^{-\frac{t^2}{\sigma^2}}$$

where σ is the shape parameter.

The procedure to calculate filter coefficients is summarized here:

(i) Compute matrix $\boldsymbol{\phi}$ whose elements are given by

$$\phi(m,k) = \varphi(|k-m|)$$

(ii) Calculate inverse matrix $\boldsymbol{\phi}^{-1}$ with elements $\alpha(n,m)$.

(iii) Obtain g weights using

$$g(m, I+kh) = \sum_{n=0}^{N} \alpha(n,m)\ \varphi(|n-I-kh|) \tag{3.10}$$

(iv) Compute a coefficients given by

$$a(k) = \frac{\Gamma(v+1)(-1)^k}{\Gamma(k+1)\Gamma(v-k+1)} \tag{3.11}$$

(v) Filter coefficients are obtained such that

$$b(m) = \frac{1}{h^v} \sum_{k=0}^{L} a(k) g(m, I+kh)$$

The method requires I as prescribed delay, v order of differentiation, large integer value L, small positive integer h for better frequency approximation. A design example with n = 61, I = 5, v = 0.5, h = 0.1, L = 620, Gaussian RBF with σ = 2.3 is demonstrated in Figure 3.10.

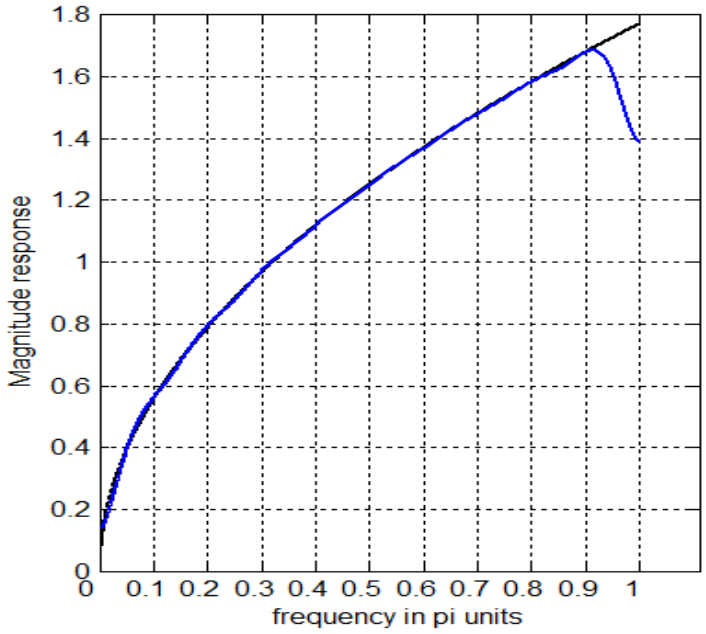

Figure 3.10: Magnitude response of designed FOD with v = 0.5 using [17]

3.3 FIR filter design

In order to find new non recursive techniques or understand some previous pioneer works of digital differentiators design understanding of basics of FIR filter design is required. FIR filter design essentially consists of two parts

(i) approximation problem

(ii) realization problem

The approximation stage takes the specification and gives a transfer function through three steps. They are as follows:

(i) A desired or ideal response is chosen, usually in the frequency domain.

(ii) An allowed class of filters is chosen (e.g. the length *N* for a FIR filters).

(iii) A measure of the quality of approximation is chosen.

The realization part deals with choosing the structure to implement the transfer function which may be in the form of circuit diagram or in the form of a program. There are essentially three well-known methods for FIR filter design namely:

(i) The window method

(ii) The frequency sampling technique

(iii) Optimal filter design methods

These methods are described in detail here.

3.3.1 The Window Method

In this method, [19], [26], [53] from the desired frequency response specification $H_d(\omega)$ corresponding unit sample response $h_d(n)$is determined using the following relation

$$h_d(n) = \frac{1}{2\pi}\int_{-\pi}^{\pi} H_d(\omega)e^{j\omega n}d\omega \tag{3.12}$$

$$H_d(\omega) = \frac{1}{2\pi}\sum_{n=-\infty}^{\infty} h_d(n)e^{-j\omega n} \tag{3.13}$$

In general, unit sample response $h_d(n)$ obtained from the above relation is infinite in duration, so it must be truncated at some point say n= M -1 to yield an FIR filter of length M (i.e. 0 to M-1). This truncation of $h_d(n)$ to length M-1 is same as multiplying $h_d(n)$ by the rectangular window defined as

$$w(n) = \begin{cases} 1 & 0 \le n \le M-1 \\ 0 & \text{otherwise} \end{cases}$$

Thus the unit sample response of the FIR filter becomes

$$h(n) = w(n)h_d(n) = \begin{cases} h_d(n) & 0 \le n \le M-1 \\ 0 & \text{otherwise} \end{cases} \tag{3.14}$$

Now, the multiplication of the window function $w(n)$ with $h_d(n)$ is equivalent to convolution of $H_d(\omega)$ with $W(\omega)$, where $W(\omega)$ is the frequency domain representation of the window function.

$$W(\omega) = \sum_{n=-\infty}^{\infty} w(n)e^{-j\omega n}$$

Thus the convolution of $H_d(\omega)$ with $W(\omega)$ yields the frequency response of the truncated FIR filter

$$H(\omega) = \int_{-\pi}^{\pi} H_d(v)W(w-v)dw$$

The frequency response can be obtained using the following relation

$$H(\omega) = \sum_{n=0}^{M-1} h(n)e^{-j\omega n} \tag{3.15}$$

But direct truncation of $h_d(n)$ to M terms to obtain $h(n)$ leads to the Gibbs phenomenon effect which manifests itself as a fixed percentage overshoot and ripple before and after an approximated discontinuity in the frequency response due to the non-uniform convergence of the Fourier series at a discontinuity. Thus the frequency response obtained by using (3.14) contains ripples in the frequency domain. In order to reduce the ripples, instead of multiplying $h_d(n)$ with a rectangular window $w(n)$, $h_d(n)$ is multiplied with a window function that contains a taper and decays toward zero gradually, instead of abruptly as it occurs in a rectangular window. As multiplication of sequences $h_d(n)$ and $w(n)$ in time domain is equivalent to convolution of $H_d(\omega)$ and $W(\omega)$ in the frequency domain, it has the effect of smoothing $H_d(\omega)$.

The several effects of windowing the Fourier coefficients of the filter on the result of the frequency response of the filter are as follows:

(i) A major effect is that discontinuities in $H(\omega)$ become transition bands between values on either side of the discontinuity.

(ii) The width of the transition bands depends on the width of the main lobe of the frequency response of the window function, $w(n)$ i.e. $W(\omega)$.

(iii) Since the filter frequency response is obtained via a convolution relation, it is clear that the resulting filters are never optimal in any sense.

(iv) Because as M (the length of the window function) increases, the mainlobe width of $W(\omega)$ is reduced which reduces the width of the transition band, but this also introduces more ripple in the frequency response.

(v) The window function eliminates the ringing effects at the bandedge and does result in lower sidelobes at the expense of an increase in the width of the transition band of the filter. Some commonly used windows are given in Table 3.1.

Kaiser Window is special because it provides control over stopband attenuation and transition width. It is given in terms of zeroth order Bessel function in (3.5). The Bartlett window reduces the overshoot in the designed filter but spreads the transition region considerably. The Hanning, Hamming and Blackman windows use progressively more complicated cosine functions to provide a smooth truncation of the ideal impulse response and a frequency response that looks better. The best window results probably come from using the Kaiser window, which has parameter β that allows adjustment of the compromise between the overshoot reduction and transition region width spreading.

The major advantages of using window method is their relative simplicity as compared to other methods and ease of use. The fact that well defined equations are often available for calculating the window coefficients has made this method successful.

There are following problems in filter design using window method:

i. This method is applicable only if $H_d(\omega)$ is absolutely integrable i.e. only if (3.12) can be evaluated. If $H_d(\omega)$ is complicated or cannot easily be put into a closed form mathematical expression, evaluation of $h_d(n)$ becomes difficult.

ii. The use of windows offers very little design flexibility e.g. in low pass filter design, the passband edge frequency generally cannot be specified exactly since the window smears the discontinuity in frequency. Thus the ideal LPF with cut-off frequency f_c, is smeared by the window to give a frequency response with

passband response with passband cutoff frequency f_1 and stopband cut-off frequency f_2.

iii. Window method is basically useful for design of prototype filter like lowpass, highpass, bandpass etc. This makes its use in speech and image processing applications very limited.

Table 3.1: Properties of commonly used Windows

Type of Window	Main Lobe Width ($\Delta\omega_M$)	Transition width($\Delta\omega$)	Relative Sibelobe Attenuation, A_{sl} (dB)	Sibelobe Attenuation, A_s (dB)
Rectangular	$4\pi/(2M+1)$	$0.92\pi/M$	13	20.9
Barlett	$4\pi/(M+1)$	$2.37\pi/M$	25	25
Hann	$8\pi/(2M+1)$	$3.11\pi/M$	31.5	43.9
Hamming	$8\pi/(2M+1)$	$3.32\pi/M$	42.7	54.5
Blackman	$12\pi/(2M+1)$	$5.56\pi/M$	58.1	75.3

3.3.2 The Frequency Sampling Technique

In this method, [19], [50] the desired frequency response is provided as in the previous method. Now the given frequency response is sampled at a set of equally spaced frequencies to obtain N samples. Thus sampling the continuous frequency response $H_d(\omega)$ at N points essentially gives us the N-point DFT of $H_d(2\pi nk/N)$. Thus by using the IDFT formula, the filter coefficients can be calculated using the following formula

$$H_d(\omega) = \frac{1}{N}\sum_{n=0}^{N-1} H(k)e^{j(2\pi n/N)k} \tag{3.16}$$

Now using the above N-point filter response, the continuous frequency response is calculated as an interpolation of the sampled frequency response. The approximation error would then be exactly zero at the sampling frequencies and would be finite in frequencies between them. The smoother the frequency response being approximated, the smaller will be the error of interpolation between the sample points. One way to reduce the error is to increase the number of frequency samples [29]. The other way to improve the quality of approximation is to make a number of frequency samples specified as unconstrained variables. The values of these unconstrained variables are generally optimized by computer to minimize some simple function of the approximation error e.g. one might choose as unconstrained variables the frequency samples that lie in a transition band between two frequency bands in which the frequency response is specified e.g. in the band between the passband and the stopband of a low pass filter.

There are two different set of frequencies that can be used for taking the samples. One set of frequency samples are at $f_k = k/N$ where k = 0,1,….,N-1. The other set of uniformly spaced frequency samples can be taken at $f_k = (k + 0.5)/N$ for k = 0,1,….,N - 1. The second set gives us the additional flexibility to specify the desired frequency response at a second possible set of frequencies. Thus a given band edge frequency may be closer to type-II frequency sampling point that to type-I in which case a type-II design would be used in optimization procedure. In a paper by [29], Rabiner has mentioned a technique based on the idea of frequency sampling to design FIR filters. The steps involved in this method suggested by Rabiner are as follows:

i. The desired magnitude response is provided along with the number of samples, N. Given N, the designer determines how fine an interpolation will be used.
ii. It was found by Rabiner that for designs they investigated, where N varied from 15 to 256, 16 N samples of $H(\omega)$ lead to reliable computations, so 16 to 1 interpolation was used.
iii. Given N values of H_k , the unit sample response of filter to be designed, $h(n)$ is calculated using the inverse FFT algorithm.

iv. To obtain values of the interpolated frequency response two procedures were suggested by Rabiner. They are :
   - $h(n)$ is rotated by $N/2$ samples(N even) or (N-1)/2 samples for N odd to remove the sharp edges of impulse response, and then 15N zero-valued samples are symmetrically placed around the impulse response.
   - $h(n)$ is cut around the $N/2nd$ sample, and 15N zero-valued samples are placed between the two pieces of the impulse response.

v. The zero augmented sequences are transformed using the FFT algorithm to give the interpolated frequency responses.

Merits of frequency sampling technique

i. Unlike the window method, this technique can be used for any given magnitude response.

ii. This method is useful for the design of non-prototype filters where the desired magnitude response can take any irregular shape. There are some disadvantages with this method i.e. the frequency response obtained by interpolation is equal to the desired frequency

3.3.3 The Optimal Filter Design Methods

Many methods are present under this category. The basic idea in each method is to design the filter coefficients again and again until a particular error is minimized. The various methods are as follows:

3.3.3.1 Least squared error frequency domain design

As seen in the previous method of frequency sampling technique there is no constraint on the response between the sample points, and poor results may be obtained. The frequency sampling technique is more of an interpolation method rather than an approximation method. This method [50] controls the response between the sample points by considering a number of sample points larger than the order of the filter. The purpose of most filters is to separate desired signals from undesired signals or noise. As the energy of the signal is related to the square of the signal, a squared error approximation criterion is appropriate

to optimize the design of the FIR filters. The frequency response of the FIR filter is given by (3.3) for a N-point FIR filter. An error function is defined as follows

$$Error(E) = \sum |H(w_k) - H_d(w_k)|^2 \tag{3.17}$$

Where $w_k = (2\,k)/L$ and $H_d(w_k)$ are L samples of the desired response, which is the error measure as a sum of the squared differences between the actual and desired frequency response over a set of L frequency samples. The method consists of the following steps:

i. First 'L' samples from the continuous frequency response are taken, where $L > N$ (length of the impulse response of filter to be designed)

ii. Then using the following formula

$$h(n) = \frac{1}{N}\sum_{n=0}^{L-1} H(k)e^{j\left(\frac{2\pi n}{N}\right)k} \tag{3.18}$$

the L-point filter impulse response is calculated.

iii. Then the obtained filter impulse response is symmetrically truncated to desired length N.

iv. The frequency response is calculated using the following relation

$$H_d(\omega) = \sum_{n=0}^{N-1} h(n)e^{-j\omega n}$$

v. The magnitude of the frequency response at these frequency points for $w_k = (2\,k)/L$ will not be equal to the desired ones, but the overall least square error will be reduced effectively this will reduce the ripple in the filter response.

To further reduce the ripple and overshoot near the band edges, a transition region will be defined with a linear transfer function. Then the L frequency samples are taken at $w_k = (2\,k)/L$ using which the first N samples of the filter are calculated using the above method. Using this method reduces the ripple in the interpolated frequency response. An

example is demonstrated in Figure 3.11, here magnitude response of a low pass filter of order 20 is plotted.

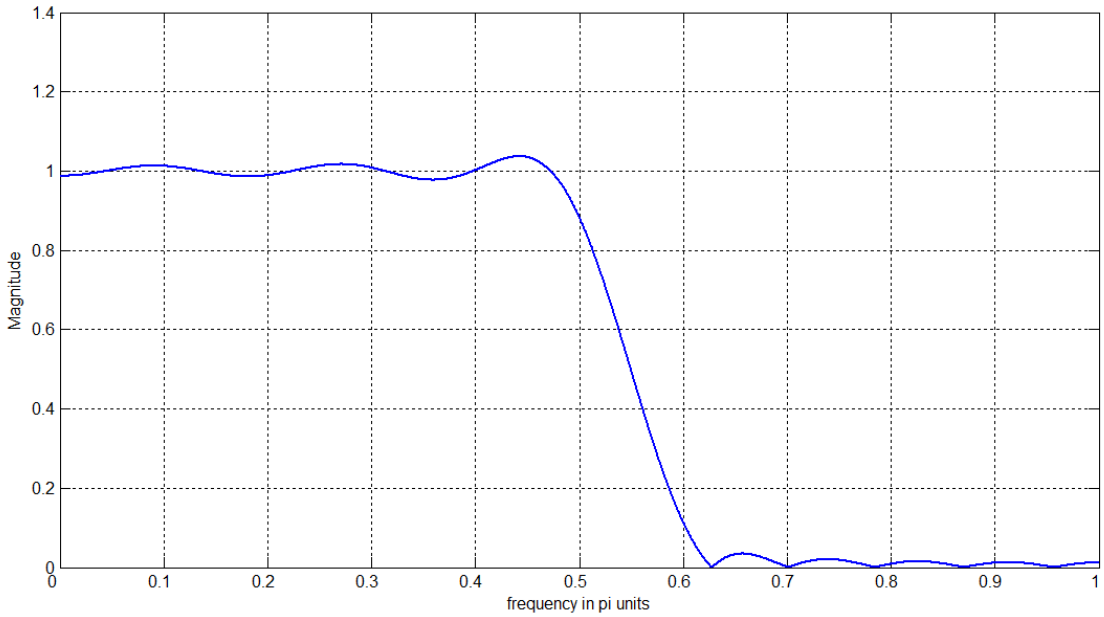

Figure 3.11: Magnitude response of Least Square method based LPF.

3.3.3.2 Parks-McClellan's Equiripple Algorithm

As we can see in Figure 1.1(b) for the filter using the Kaiser window, the stopband has ripple that generally decreases. In fact, if the passband characteristic were magnified, we would see ripple there as well. Both the passband and stopband ripple (error) tend to be larger near the transition bands and then taper off as the response moves away from the band edge. This type of response is not optimum. An optimum filter would have ripple in the passband and stopband with a constant maximum magnitude. The error would still be present but would be distributed equally throughout the bands. In this section, we discuss a method for designing FIR filters with this characteristic. The Parks-McClellan algorithm, as it is generally known, was first presented nearly 30 years ago. A primary component of the PM algorithm is a technique called the Remez exchange algorithm. But before we can use the power of the Remez algorithm to optimize our FIR filter coefficients, we must redefine our problem in such a way that the solution requires the minimization of an error function. To that end, we first define the frequency response of an odd-order FIR filter with symmetrical coefficients $h(n)$.

$$C(\omega) = \sum_{m=0}^{M} c(m)\cos(\omega)$$

The error function can be described in terms of the desired frequency response $e^{-j\omega M}\, D(\omega)$, the actual frequency response $e^{-j\omega M}\, C(\omega)$, and a weighting function $W(\omega)$ that can be used to adjust the amount of error in each filter band, such that

$$E(\omega) = W(\omega)[D(\omega) - C(\omega)]$$

If we pick a set of frequencies ($x = M + 1$) at which the extremes of the error occur, above equation can be written as

$$E(\omega_i) = W(\omega_i)[D(\omega_i) - C(\omega_i)] \tag{3.19}$$

This equation can be expanded into matrix form by considering only $x + 1$ frequencies.

$$\begin{bmatrix} 1 & \cos(\omega_0) & \cdots & \cos(M\omega_0)/W(\omega_0) \\ 1 & \cos(\omega_1) & \cdots & (-1)\ \cos(M\omega_0)/W(\omega_0) \\ \vdots & \vdots & \vdots & \vdots \\ 1 & \cos(\omega_x) & \cdots & (-1)^x \cos(M\omega_x)/W(\omega_x) \end{bmatrix} \begin{bmatrix} c(0) \\ c(1) \\ \vdots \\ c(M) \\ \delta \end{bmatrix} = \begin{bmatrix} D(\omega_0) \\ D(\omega_1) \\ \vdots \\ D(\omega_{x-1}) \\ D(\omega_x) \end{bmatrix}$$

ω_0 to ω_x represents the extremal frequencies and δ is the error. With this expression the filter design problem has been set into a form that can be manipulated by the Remez exchange algorithm. The Remez exchange algorithm is a powerful procedure that uses iteration techniques to solve a variety of minimax problems. a set of discrete frequency points is defined for the passband and stopband of the filter. (Transition bands are excluded.) This dense grid of frequencies is used to represent the continuous frequency spectrum. Extremal frequencies will then be located at particular grid frequencies as determined by the algorithm. The basic steps of the method as it is applied to our filter design problem are shown below.

Step I. Make an initial guess as to the location of $x + 1$ extremal frequencies, including an extremal at each band edge.

Step II. Using the extremal frequencies, estimate the actual frequency response by using the Lagrange interpolation formula.

Step III. Locate the points in the frequency response where maximums occur and determine the error at those points.

Step IV. Ignore all new extremals beyond the number initially set in I.

Step V. If the difference between the maximum and minimum error at the remaining extremal is small enough, continue to VI. Otherwise return to II using the retained extremals.

Step VI. Estimate the final frequency response and determine the $c(m)$ values from it. Then determine the impulse response coefficients.

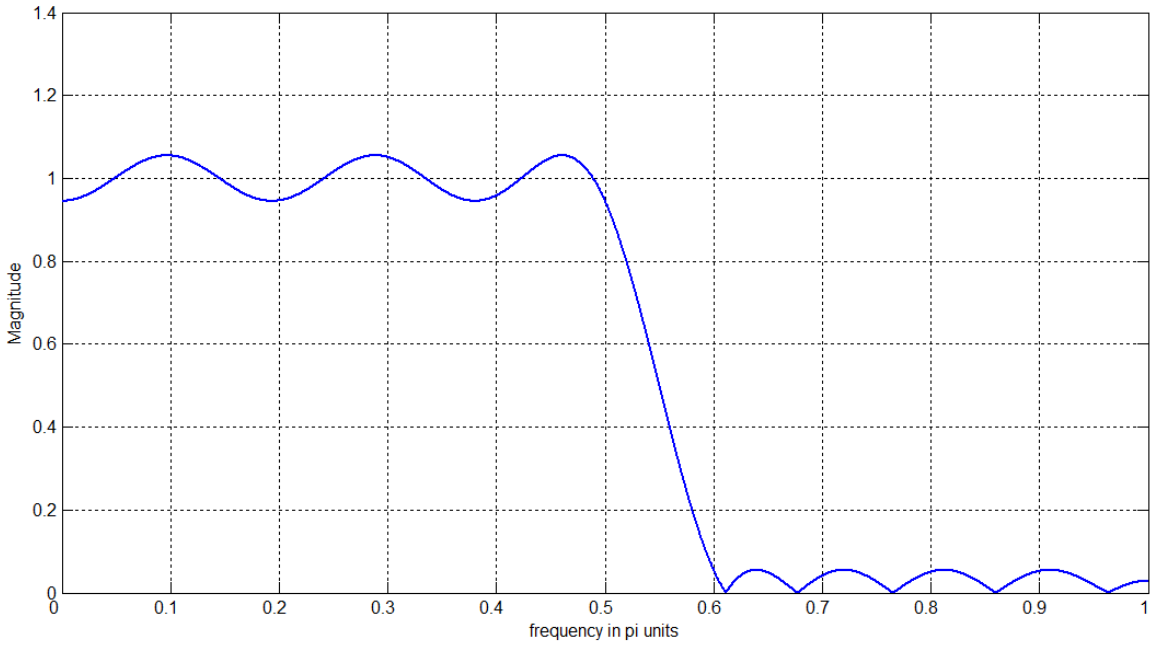

Figure 3.12: Magnitude response of equiripple method based LPF.

The simplest method of implementing step I is to assign the $x + 1$ extremal frequencies such that they are equally spaced throughout the bands of interest. Extremals are usually placed at all band edges that are adjacent to transition bands. In step V, we check the difference between the largest and smallest error produced at the retained extremals. By using this value as a progress indicator, we can set some threshold to indicate when the

procedure has produced the required level of optimization. If the differences between the minimum and maximum errors have not been reduced enough, the algorithm continues from step II. When the optimization procedure has reached the desired threshold, the extremal frequencies can be used to determine the $c(m)$ and therefore the impulse response coefficients $h(n)$. An example LPF magnitude response is illustrated in Figure 3.12. The length of impulse response taken here is 20.

3.4 Summary

The chapter describes the various techniques involved in the design of Digital Differentiators and FIR filters. Various methods to design differentiators, whether they are low pass, full band or fractional order, are explored. First, full band first order digital differentiator is analyzed and different design examples are produced. Then, Salesnick;s and Alaoui's approaches to design LPDDs are discussed in detail and compared briefly. It is observed that Alaoui's recursive LPDD has less transition width and overshoot. Design procedures using frequency approximation and Radial Basis Functions are discussed along with design examples for FODs. Various FIR filter design methods' overview is given later in the chapter. Every method has its own advantages and disadvantages and is selected depending on the type of filter to be designed. The window method is basically used for the design of prototype filters like the low-pass, high-pass, band-pass etc. They are not very suitable for designing of filters with any given frequency response. On the other hand, the frequency sampling technique is suitable for designing of filters with a given magnitude response. The ideal frequency response of the filter is approximated by placing appropriate frequency samples in the z plane and then calculating the filter coefficients using the IFFT algorithm. The disadvantage of the frequency sampling technique was that the frequency response gave errors at the points where it was not sampled. In order to reduce these errors the different optimization technique for FIR filter design were presented wherein the remaining frequency samples are chosen to satisfy an optimization criterion.

Chapter –4

Higher Order Low Pass Digital Differentiators

4.1 Introduction

This chapter describes the design of linear phase FIR higher order low pass digital differentiators. An expression is introduced, to calculate impulse response coefficients, by using Fourier series design method. Then window filter design technique is employed along with Kaiser Window to design filters.

Higher order low pass digital differentiators are used to avoid unwanted amplification of noise, as in case of full band ones [24]. Salesnick provided recursive formula to design first order FIR low pass differentiator's impulse response coefficients in [24]. Alaoui described the recursive design procedure of low pass differentiators in [31]. Alaoui's approach proved to be better in transition width as compared to Salesnick's method. Higher order differentiation is an important signal processing technique, found in many applications such as biomedical signal processing and calculations of geometric moments [49]. Low pass differentiator can be implemented by a single filter or with cascading of differentiator and low pass filter [31]. The frequency response of higher order ideal full band differentiator is given by

$$H(\omega) = (j\omega)^{v} \text{ for } |\omega| < \pi$$

where v is a natural number for higher order case of differentiators.

The higher order low pass differentiator is characterized by ideal frequency response as

$$H_{LP}(j\omega) = \begin{cases} j\omega^{v} & , \quad |\omega| \le \omega_c \\ 0 & , \quad \omega_c \le |\omega| \le \pi \end{cases} \tag{4.1}$$

where $\omega_s = 2\pi$ is the sampling frequency in radians per second. Here ω_c is cutoff frequency such that $\omega_k = k\pi$, k is the parameter to control cutoff frequency in designing practical low pass differentiators.

Electrocardiogram (ECG) provides useful information of the condition of heart. Most automatic ECG diagnosis techniques require an accurate detection of the QRS complexes. An application in the form of QRS complex detection is discussed at the end of chapter. ECG recorded from a patient with heart disease often exhibits abnormal characteristic waves. Automatic analysis and classification of ECG can ease the burden of cardiologist and speed up the diagnosis [38], [40] and [43]. Accurate QRS complex detection is important in R peak detection and R-R interval extraction from ECG. An improvement in existing second derivative QRS complex detection methods could be achieved by using higher order low pass differentiators. First order differentiation is preferred over higher order differentiation because of low complexity requirements. Especially in real time implementation of the system.

4.2 Higher Order Low Pass Digital Differentiator

Impulse response coefficients of the differentiator is calculated by using Fourier series technique of filter design [26], [50], [53], expressed as

$$h(n) = \int_{-\pi}^{\pi} H(\omega) e^{j\omega n} d\omega \tag{4.2}$$

Using (4.1) and from [41], the integral can be written as

$$h(n) = \left[\frac{e^{j\omega n}}{n} \left\{ (j\omega)^{v} - \frac{v}{n}(j\omega)^{v-1} + \frac{v(v-1)}{n^2}(j\omega)^{v-2} - \cdots \right\} \right]_{-k\pi}^{k\pi}$$

$$h(n) = \left[\frac{e^{j\omega n}}{n} \sum_{q=0}^{v} \frac{v!\,(j\omega)^{v-q}(-1)^{q}}{(v-k)!\,n^{q}} \right]_{-k\pi}^{k\pi}$$

let $l = v - q$, then

$$h(n) = \left[\frac{e^{j\omega n} v!\,(-1)^{v}}{n^{v+1}} \sum_{l=0}^{v} \frac{(-j\omega n)^{l}}{l!} \right]_{-k\pi}^{k\pi}$$

$$= \left[\left(\frac{-1}{n}\right)^{v} \frac{e^{j\omega n} v!}{n} \sum_{l=0}^{v} \frac{(-j\omega n)^{l}}{l!}\right]_{-k\pi}^{k\pi}$$

$$= \left[\left(\frac{-1}{n}\right)^{v} \frac{1}{n} \Gamma(v+1, -j\omega n)\right]_{-k\pi}^{k\pi}$$

$$= \left(\frac{-1}{n}\right)^{v} \frac{1}{n} \{\Gamma(v+1, -jk\pi n) - \Gamma(v+1, jk\pi n)\} \tag{4.3}$$

So the discrete time system is obtained as

$$H(z) = \sum_{n=-N1}^{N1} h(n) z^{-n} \tag{4.4}$$

The amplitude response of ideal digital differentiator is

$$H_i(\omega) = |\omega|$$

Then amplitude response of the designed differentiator is given by

$$H_d(\omega) = \left| \sum_{n=-N1}^{N1} h(n) e^{-j\omega n} \right|$$

The error in amplitude response of designed digital differentiator is

$$E(\omega) = H_d(\omega) - H_i(\omega) \tag{4.5}$$

The impulse response of a first order digital differentiator is shown in Figure. 4.1. In order to obtain finite length of impulse response, the Fourier series is truncated such that

$$h(n) = 0 \text{ for } |n| > (N-1)/2$$

where N is length of the filter and an odd integer.

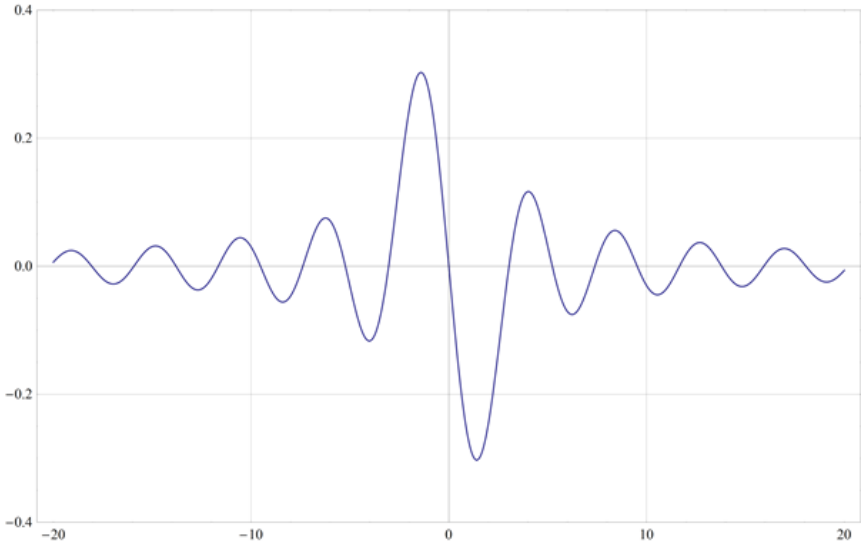

Figure 4.1: Impulse response plot of an HOD with k = 0.35, v= 1

Due to truncation of Fourier series, Gibbs oscillations are introduced in the frequency response of the differentiator. These oscillations' amplitude can be reduced by the use of window functions [1], [6]. This preconditioning result in transfer function of the filter given by

$$H(z) = \sum_{n} (w(nT)h(nT))z^{-n} \tag{4.6}$$

Here Kaiser window is used as it provides extra degree of freedom by providing shaping parameter α. This feature of Kaiser Window helps in the designing process of digital differentiator [1], [2]. Kaiser window function is given by following expression

$$w(n) = \frac{I_0(\alpha\sqrt{1-(n/N_1)^2})}{I_0(\alpha)} \; ; \; -N_1 \leq n \leq N_1 \tag{4.7}$$

where $N_1 = (N-1)/2$ and I_0 is zeroth order Bessel function of first kind.

A parameter $L(\alpha, N)$ can be defined as maximum error in passband of the practical digital differentiator, such that

$$L(\alpha, N) = \max|E(\omega)| \quad \text{for} \quad 0 \leq \omega \leq \omega_c \tag{4.8}$$

In order to achieve minimum of $L(\alpha, N)$ with respect to α, this optimum value can be calculated from an optimization procedure consisting of a combination of golden section search and successive parabolic interpolation as given in [39] and [42]. This algorithm requires three parameters, an initial interval of values of α and tolerance. The working of algorithm is reduction of the interval of uncertainty, on each iteration, by the factor 0.618, until it is less than the tolerance. Therefore it is better than bisection based counterparts. This method is faster computationally and is used to find optimum value of α in design examples of this chapter.

4.3. First Oder Low Pass Differentiator

The design process can be categorized into three parts, such that the differentiator is designed for given specifications. Different design options are discussed in this section separately. So, this approach allows flexibility to optimize desired parameters according to provided specifications.

4.3.1. Differentiator design with minimum passband error for a given value of N

Optimum value of α is found using the optimization algorithm for provided N. Once we know N, α and v the differentiator can be designed by using (4.6). Some results of the algorithm are given in Table 4.1, rows and columns show progression of optimization procedure for N = 29, v= 1 and ω_c= 0.35 π.

Table 4.1: Progress chart of optimization algorithm to design first order LPDD

N	α^*	$L(\alpha^*, N)$	Number of Iterations
25	4.44	0.0051	10
31	5.6	0.0016	10
39	7.16	0.00034	11

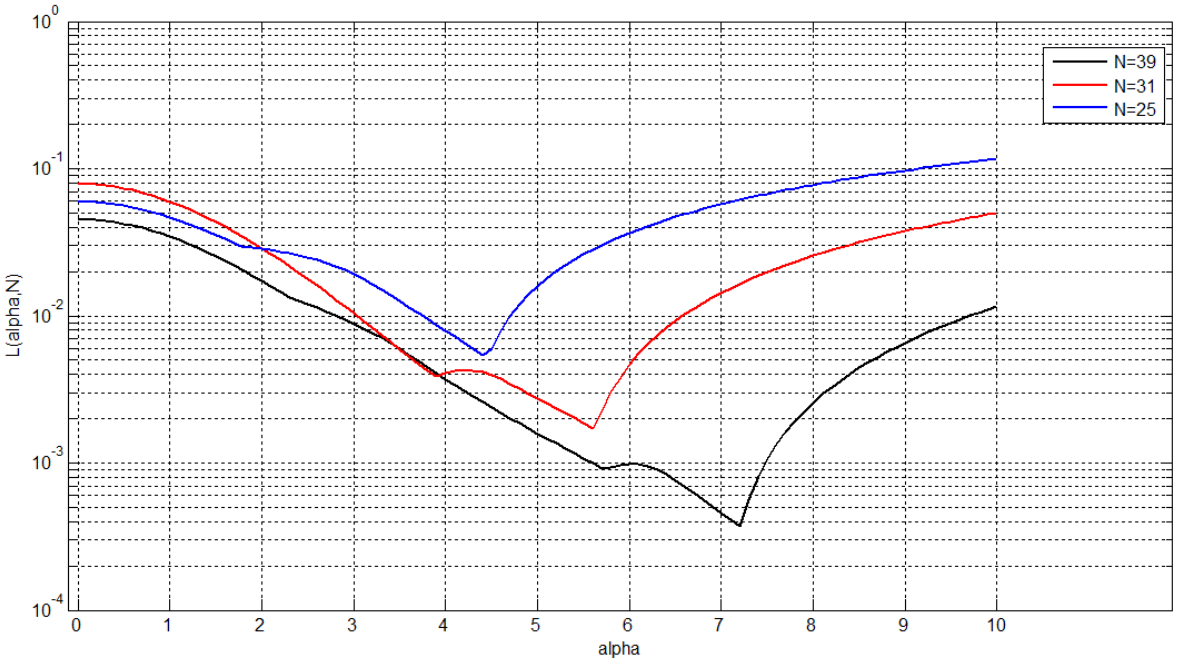

Figure 4.2: $L(\alpha, N)$ curve for $\omega_c = 0.35\pi$ and $v = 1$.

4.3.2. Differentiator design with minimum N for a provided in band error δ

An important observation from Figure 4.2 and Table 4.1 is linearity in plot as N is increased. This linearity in plots of $\ln(e/e_1)$ against $N - N_1$ for different values of N_1 [2] can be exploited, to calculate value of N only by two minimizations. As it can be seen in Figure 4.2, global minima points almost lie on a straight line.

Minimum value of N which achieves the specified inband error can be calculated by procedure given in [2]. In this method if

$$e = L(\alpha^*, N) \quad \text{and} \quad e_1 = L(\alpha^*{}_1, N_1)$$

where $\alpha_1{}^*$ and α^* are global minima point for N_1 and N respectively of designed digital differentiator for a particular normalized cutoff frequency ω_c, then

$$N = N_1 + \frac{\ln(e/e_1)}{\ln(e_2/e_1)}(N_2 - N_1) \tag{4.9}$$

This formula calculates N such that it satisfies user requirement given by

$$L(\alpha^*, N) \leq \delta$$

where δ is maximum acceptable error in passband of low pass digital differentiator.

For example, if ω_c= 0.35 then by using optimization procedure described in previous section, ${\alpha_1}^*$ and ${\alpha_2}^*$ are computed for N_1= 25 and N_2= 29 with δ taken as 0.0005. Then following results are obtained

$$N_1 = 25\ {\alpha_1}^* = 4.44\ e_1 = 0.0051$$

$$N_2 = 29\ {\alpha_2}^* = 5.6\ \ e_2 = 0.0016$$

It yields N = 39 and e comes out less than 0.0004.

4.3.3 Differentiator design with given in band accuracy and N to obtain minimum transition width

In many applications error of 2% is acceptable in passband of low pass differentiator; therefore transition width can be optimized under this constraint. Salesnick's and Alaoui's approaches are compared with the Fourier series technique as in Figure 4.3 and Figure 4.4. It can be seen that designed differentiator's response is better in terms of transition region and sharp cut off characteristics. These features are important for suppression of high frequency noise. The overshoot, present in the amplitude response after reaching ω_c, decreases as α increases but so does error in passband. A relatively higher value of α is selected for minimum overshoot under 2% constraint as shown in Figure 4.3. In this case α is taken 6.6.

4.4 Second Order Low Pass Differentiator

To obtain good performance at zero normalized frequency a constraint on coefficients is imposed, [23] so that

$$\sum_{n=-N_1}^{N_1} h(n) = 0$$

Same options as in first order case can also be taken here as well.

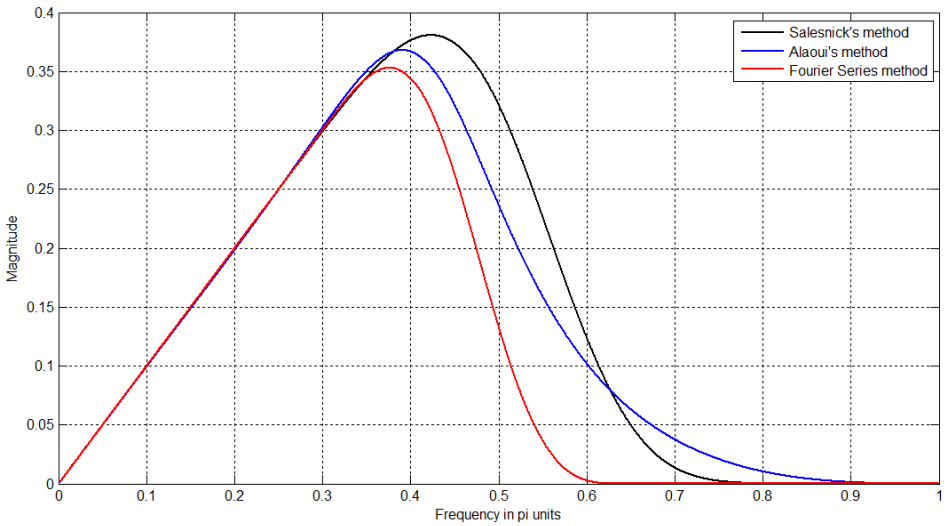

Figure 4.3: Magnitude comparison of Salesnick's, Alaoui's and Fourier Series methods of first order LPDD design for ω_c = 0.35

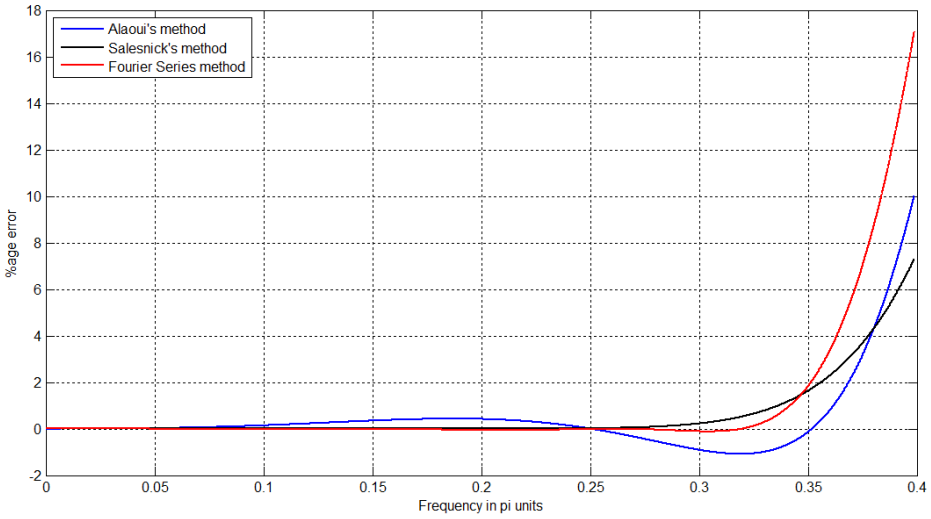

Figure 4.4: Error comparison of Salesnick's, Alaoui's and Fourier Series methods of first order LPDD design for ω_c = 0.35 in passband

4.4.1 Differentiator design with minimum passband error for a given value of N

Optimum α is found using golden section optimization and progress chart of some of them is provided in Table 4.2.

Table 4.2: Progress chart to design second order LPDD for ω_c= 0.35π and N = 29

N	α^*	$L(\alpha^*, N)$	Number of Iterations
25	4.42	0.00757	10
31	5.55	0.00245	11
39	7.11	0.00047	10

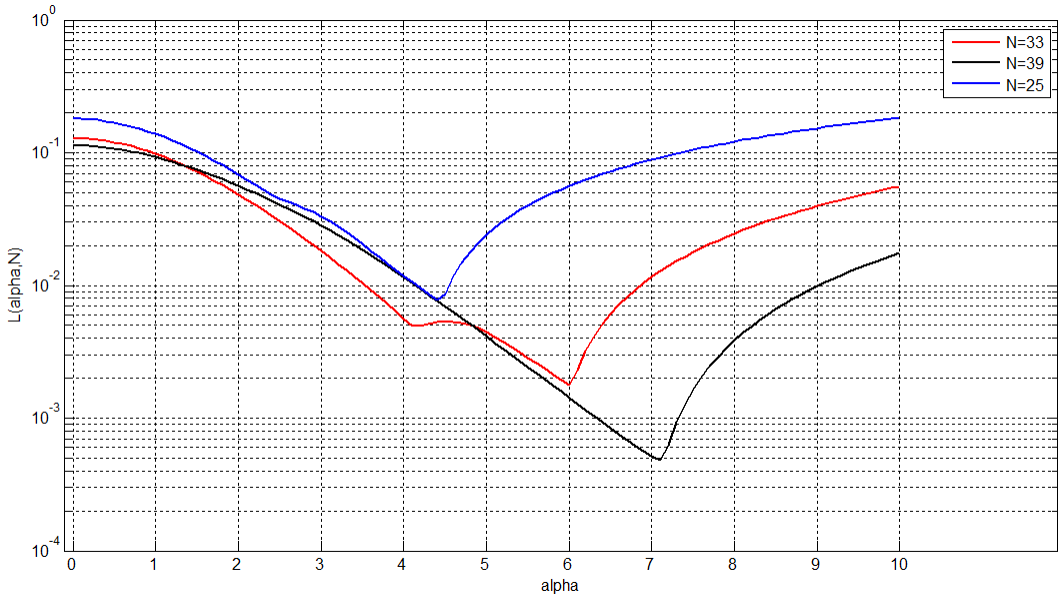

Figure 4.5: $L(\alpha, N)$ curve for different filter lengths k = 0.35 and v = 2

4.4.2 Differentiator design with minimum N for a provided in band error δ

Linearity in plots of $\ln(e/e_1)$ against $N - N_1$ for different values of N_1 is present in second order differentiator also, as can be seen in Figure 4.5. Therefore the procedure to design differentiator with minimum N could be applied in this case also for given δ. It can be easily verified by checking Table 4.2 and taking δ as 0.0005.

4.4.3 Differentiator design with given in band accuracy and N to obtain minimum transition width

As discussed in last section amplitude response can be optimized to attain given accuracy in passband. This feature is due to the fact that α can be varied to any fractional value as opposed to Salesnick's approach. The Figure 4.6 shows the amplitude response of differentiator of impulse response length 29 and normalized cut off frequency 0.55π with applied constraint of 2%. α has value of 5.5. Percentage error plotted in Figure 4.7 of the designed differentiator shows in band error is less than specified constraint.

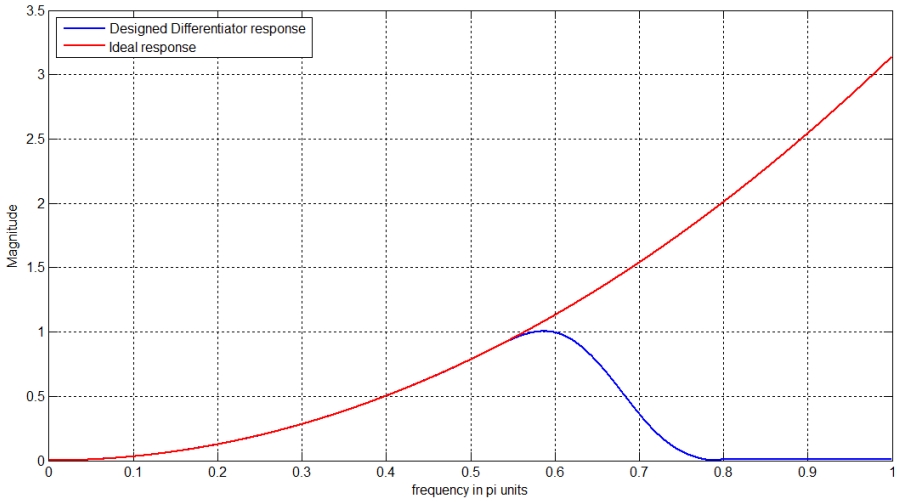

Figure 4.6: Frequency response of Fourier Series LPDD for v = 2, ω_c= 0.55 and N = 29

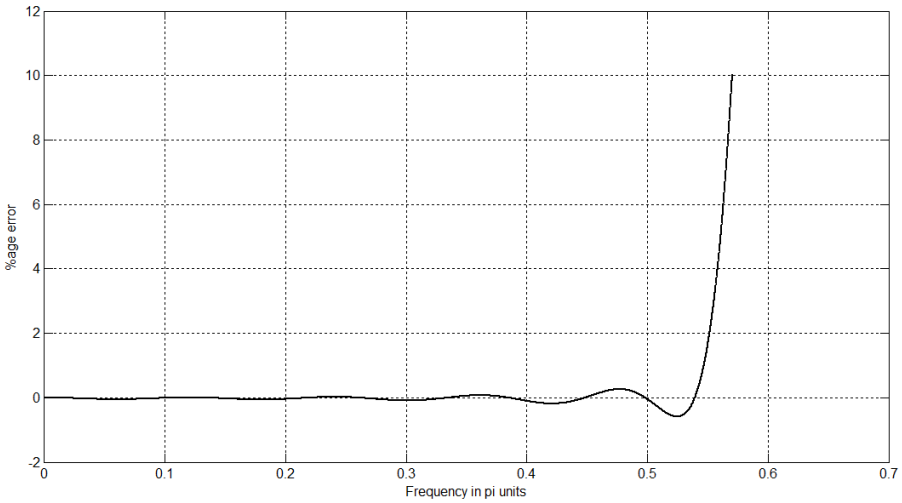

Figure 4.7: Percentage error of Fourier Series LPDD for v = 2, ω_c= 0.55 and N = 29

Same technique for different values of ω_c is illustrated in Figure 4.8. The flexibility provided by α can also be observed in this plot. By changing it to suitable value, desired cutoff characteristics are achieved in frequency response.

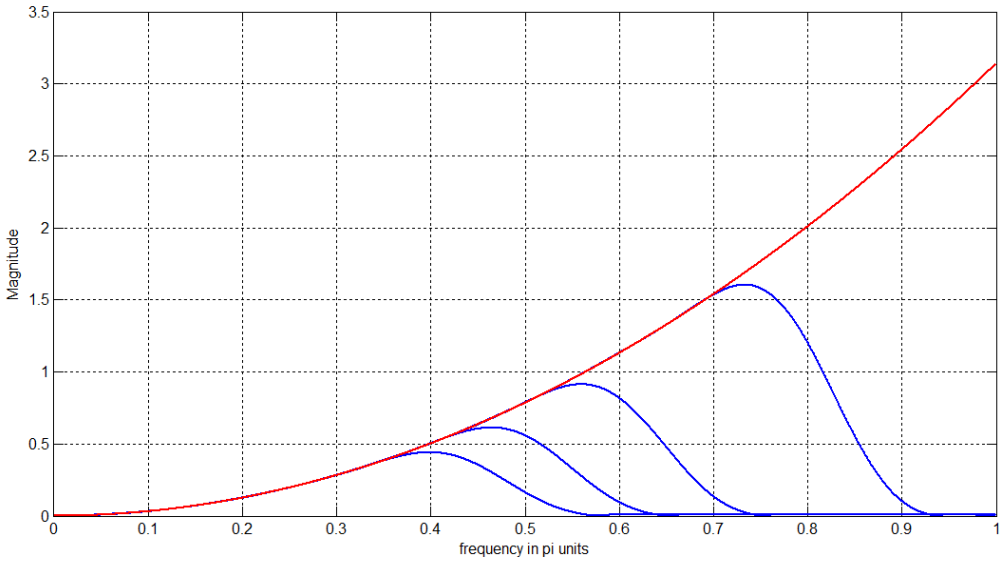

Figure 4.8: Magnitude response for v = 2, N = 29 and ω_c= 0.35π, 0.42π, 0.52π, 0.7π

4.5 QRS Complex Detection

In this section an application of higher order FIR low pass differentiator is demonstrated. Algorithms based on derivatives are suitable for real time applications [38]. It illustrates the use of these filters in biomedical signal processing, where low frequency components of signal are important. QRS complex detection is needed in beat and beat-to-beat interval information in an electrocardiogram (ECG) recording [38]. It is crucial to accurately detect QRS, as it contains P and T wave, as well as noises [40] and artifacts as described here. An ECG with such distortions is shown in Figure 4.11 (a). Various reasons for ECG signal distortion are

(i) Power line interference consisting of 60 Hz frequency and harmonics.
(ii) Electromyographic interference, which is random high frequency noise.
(iii) Baseline drift due to respiration or abrupt shift in baseline.

Second derivative based method, as described in [38], is used here. The structure of the technique is shown in Figure 4.9. A Kaiser window based FIR band pass filter is

employed to pass the QRS complex frequencies such that 8 to 20 Hz passband. First differentiator is a center differentiation stage and second differentiator is forward differentiation stage. Zero crossings are formed in the locations of R waves after first differentiation process, therefore another differentiation is required to form peaks at R waves. This introduces delay in the sequence. The second differentiator stage presents a filter with odd phase and high-pass frequency response

$$D\left(e^{j\omega}\right) = e^{j\omega} - 1$$

$$D\left(e^{j\omega}\right) = \sqrt{2 - 2\cos(\omega)}$$

This method rectifies the signal by its odd-phase property, resulting in a large local minimum at each QRS complex. The odd-phase and high-pass filter properties of the second differentiation stage results in nonuniform filtering of the low and high frequency components of the differentiated ECG. However, since the ECG has already been low-pass filtered, additional filtering by this method will further attenuate the QRS complexes.

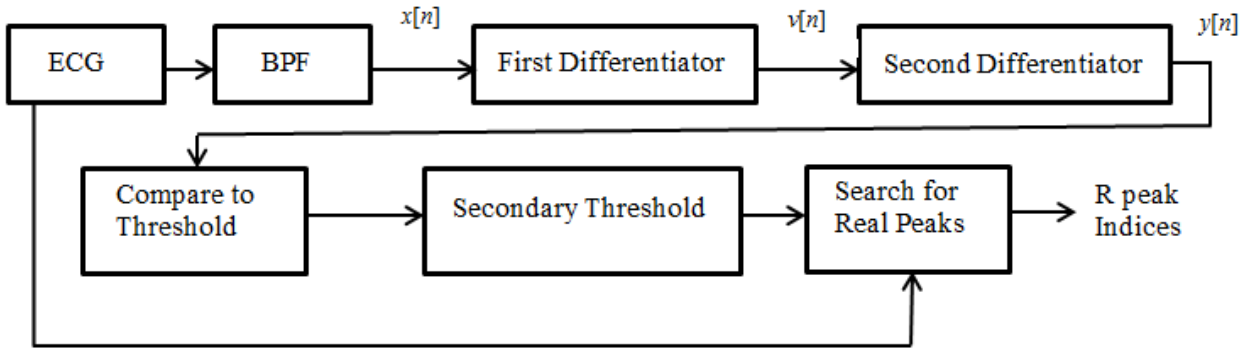

Figure 4.9: Second derivative method (the first technique) structure for QRS complex detection [38]

The adaptive threshold is computed from root mean squared (RMS) value of a data segment. In the end, if a peak is detected then a search back algorithm is used, it based on 200 ms physiological refractory period before another QRS complex can occur. Therefore another peak present in 200 ms window is stored for further analysis.

Digital differentiators are high pass filters and their low pass case can be considered as a band pass filter, especially at higher order differentiation. The structure of this technique

is modified such that band pass filter is no longer used and there is also no need of second stage of differentiation. Therefore the first three stages of the structure are highly simplified due to second order low pass differentiator as given in Figure 4.10. The output is directly obtained from a filter as opposed to three stages (with complexity equivalent to first stage of s) in the case of first technique.

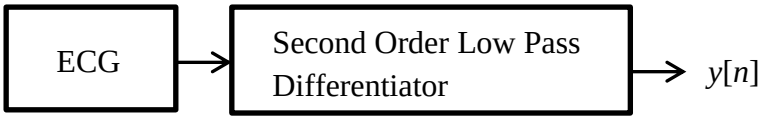

Figure 4.10: The proposed low pass differentiator method (the second technique) structure

This methodology was applied on MIT/BIH arrhythmia database [5]. These ECG recordings have been sampled at 360 Hz with 11 bit resolution over the range of 10 mV. Record 108 is used in this section to illuminate the proposed algorithm's performance. This recording has rare long P waves and high noise contents [4], it has reversed polarity QRS complexes. The second order FIR differentiator's impulse response length is 35 and window parameter is taken 6.33 (from optimization algorithm). The number of coefficients in bandpass filter is also 35. The resultant output, $y[n]$, from both the arrangements is plotted in Figure 4.11.

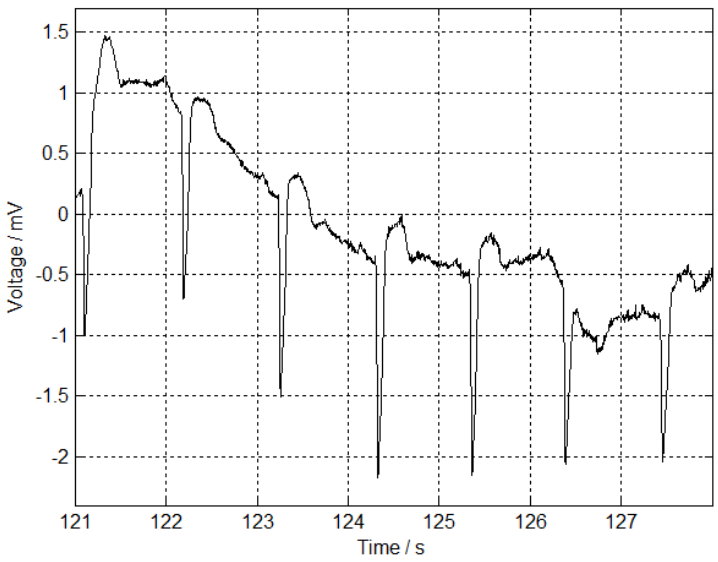

(a)

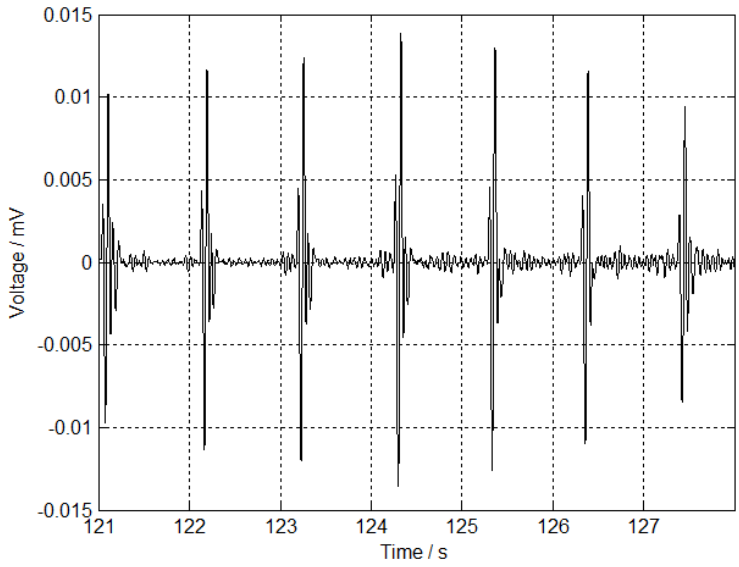

(b)

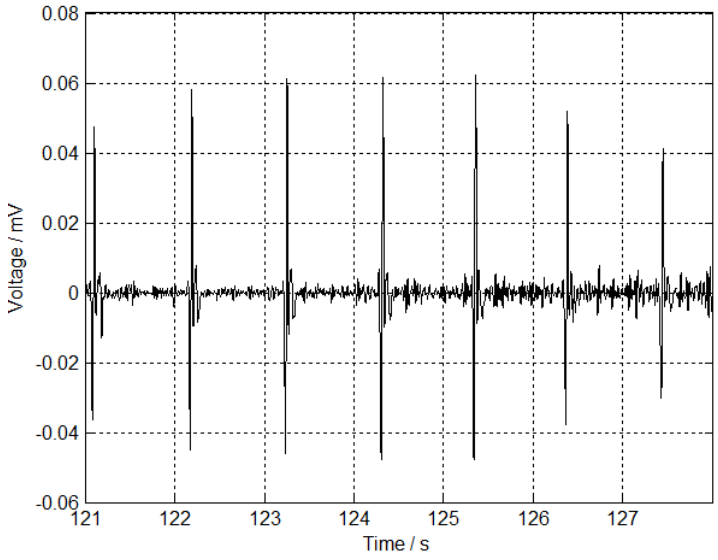

(c)

Figure 4.11: ECG processing results (a) ECG signal from Record 108 (b) $y[n]$ output from first algorithm (c) $y[n]$ output from proposed algorithm

The second derivative method produces peaks with more gradual transition from zero voltage, as given in Figure 4.11 (b). The proposed algorithm exhibits sharp outstanding peaks in the location of R peaks, as illustrated in Figure 4.11 (c). It should also be noted that number of coefficients in bandpass filter, of first technique, is the same as number of

coefficients in second order low pass differentiator of the second technique. First method requires two stages of differentiation after the filter, however this method embeds the three operations in the filter of same length. Therefore number of operations required by the proposed method to detect QRS complex are reduced. This feature is crucial in real time implementation of QRS detection of patient's ECG and Holter tape monitoring [43] also. Although here we have presented QRS complex detection application, the proposed approach can be employed in second derivative based biomedical signal processing.

4.6 Summary

In this chapter, we described the design of higher order case of FIR low pass digital differentiators. The impulse response coefficients of the differentiator are derived using Fourier integral.

This expression is used to design first order differentiator with varying normalized cutoff frequency using Kaiser Window. It provides an easy way to change cutoff frequency without altering the sampling frequency, reducing aliasing risk in the system. The frequency response of designed differentiator is compared with Salesnick's [24] and Alaoui's [31] approaches. The proposed differentiator is having shorter transition regions and less overshoot in frequency response. Flexibility in design process is observed due to possibility of window shaping parameter to fractions. Second order differentiators are produced and error analysis is illustrated by graphs. Different design options available to user due to window shaping parameter are discussed separately.

The formula is employed to obtain second order FIR low pass differentiator for QRS detection in ECG. The proposed algorithm enables us to detect R peaks even in presence of noise and baseline wanders, as demonstrated by using MIT/BIH ECG recording. This technique also has low complexity as compared to second derivative counterparts, which makes it suitable for real time processing of ECG waveform. This method could well be used in second derivative based biomedical signal processing at a lower computational cost.

Chapter –5

Linear Phase FIR Fractional Order Differentiator Design

5.1 Introduction

Convex optimization has been discussed in detail in chapter 1. It was used to design magnitude frequency response using spectal factorization in [7]. Because FIR filter magnitude design is not convex optimization problem, therefore it is converted into one by using change of variables. However, linear phase FIR filter design is a convex problem as they have symmetry or anti symmetry in their impulse response. Design process is highly simplified by convex optimization based design process. It is by virtue of spectral constraint and minmax (Chebyshev) based problem formulation.

FIR filters are characterized by following equation

$$y(t) = \sum_{k=0}^{n-1} h(k)x(t-k) \tag{5.1}$$

where x is input signal and h is impulse response. So, they are linear systems described by convolution relation in input and output [6], [19]. Its frequency response is given by

$$H\left(e^{j\omega}\right) = \sum_{k=0}^{n-1} h(k)e^{-j\omega k} \tag{5.2}$$

It can also be written as vector product as in [3]

$$H\left(e^{j\omega}\right) = \boldsymbol{v}^H \boldsymbol{h} \tag{5.3}$$

The vector $[\boldsymbol{v}]_{\boldsymbol{k}} = e^{j\omega k}$ and $\boldsymbol{h}$ contains real valued filter coefficients. FIR filters has the advantage of linear phase if filter coefficients are symmetric or anti-symmetric about its center point. Then the frequency response of linear phase filter can be expressed as

$$H\left(e^{j\omega}\right) = e^{j\theta(\omega)}\, \widetilde{H}\left(e^{j\omega}\right) \tag{5.4}$$

where $\widetilde{H}(e^{j\omega})$ is amplitude response of such that

$$\widetilde{H}(e^{j\omega}) = \widetilde{\boldsymbol{v}}^T \widetilde{\boldsymbol{h}} \tag{5.5}$$

$\widetilde{\boldsymbol{h}}$ is half of impulse response and $\theta(\omega) = \theta_0 + \mu(\omega)$

The parameters θ_0 and μ depend on length of impulse response and type of FIR linear phase filter [52]. These parameters for the four type of filters are given by

Table 5.1: Properties of different types of FIR linear phase filters

	$\mu(\omega)$	θ_0	$\widetilde{\boldsymbol{v}}$
Type I	$n/2$	0	$[1 \;\; 2cos(n\omega)]$
Type II	$n/2$	$-\pi/2$	$[2cos\left(\left(n-\frac{1}{2}\right)\omega\right)]$
Type III	$n/2$	0	$[2sin(n\omega)]$
Type IV	$n/2$	$-\pi/2$	$[2sin\left(\left(n-\frac{1}{2}\right)\omega\right)]$

Optimization design of FIR filters is carried out by using two steps. First, characteristic specification by equality or inequality constrains. Then optimal value of a chosen performance metric is calculated using the optimization procedure. The problem can be very difficult to solve but if inequality constrains are convex and equality constrains are affine then any local optimum is global optimum. This highly simplifies the task. Software tools (e.g. [25] and [36]) are available to find global optimum with a little programming. Recently, algorithms are developed that solve convex problems very efficiently [44]. The tools available easily detect infeasibility arising from no solution to the problem. FIR filter design problems are convex optimization problems when

symmetry constraints are imposed e.g. in the case of linear phase filter design. A design example is a first order low pass digital differentiator that minimizes passband error. This optimization problem can be expressed as

$$\begin{aligned} &\textit{minimize} && \alpha \\ &\textit{subject to} && \omega + \alpha \le H(\omega) \le \omega - \alpha \qquad \omega \in [0, \omega_p] \\ & && H(\omega) \le \delta \qquad\quad \omega \in [\omega_s, \pi] \end{aligned} \tag{5.6}$$

where filter coefficients, $\boldsymbol{h} \in \boldsymbol{R}^n$, and passband ripple α are optimization variables. ω_p, ω_s, filter order n, stopband attenuation δ are problem parameters. Passband ripple and stopband attenuation can be expressed in decibels i.e. as $20\ log_{10}(\alpha)$ and $20\ log_{10}(\delta)$.

The above problem formulation contains semi-infinite inequality constraints [7]. These can be approximated by using frequency sampling. It is done by taking a set of frequencies in $\omega \in [0, \omega_p]$, i.e.

$$0 \le \omega_1 \le \omega_2 \ldots . \le \omega_N \le \omega_p$$

or in $\omega \in [\omega_s, \pi]$ as required. Then we can replace semi-infinite inequality constraints with N inequality constraints because sampling preserves convexity [7]. $N = 15\ n$ is taken here to design examples.

5.2 Low Pass Digital Differentiators

The design process of low pass differentiators can be categorized into three parts, such that the differentiator is designed for given specifications. In the following sections linear phase FIR type III digital differentiators are designed for first order case.

5.2.1 Differentiator design with minimum passband error (α).

The problem statement is same as (5.6). Here the optimization variables are δ and $\boldsymbol{h}$. An example design, with above described approach, is shown in Figure 5.1. Error in passband is plotted in Figure 5.2. The filter order is n = 43, passband frequency is ω_p = 0.4 π and stopband frequency is ω_s = 0.55 π, stopband attenuation is taken as 50 dB. No constraints are imposed on magnitude response in transition region.

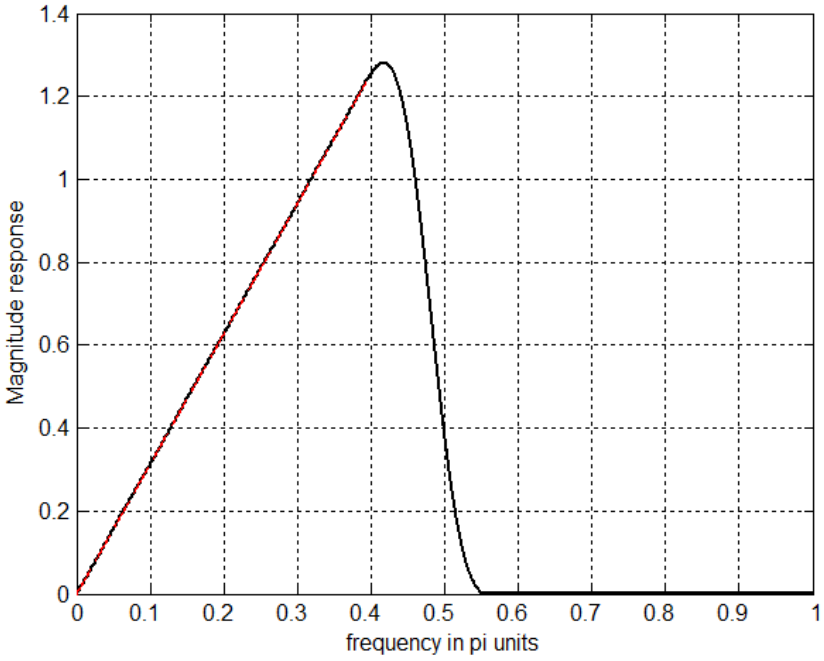

(a)

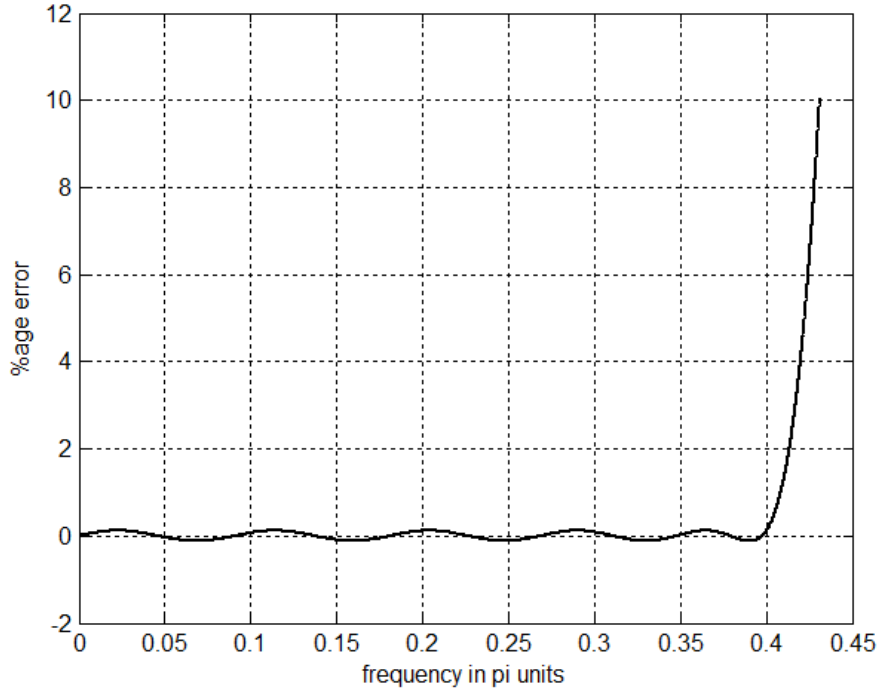

(b)

Figure 5.1: Convex optimization based first order LPDD (a) Magnitude Response (b) Error Plot

5.2.2 Differentiator design with minimum transition width

The problem of minimizing transition width (i.e. ω_s) is quasiconvex [7], it can be effectively solved by applying bisection on ω_s and keeping other parameters fixed. The optimization specifications are same as (5.6). The design parameters taken are specifications n = 29, ω_p = 0.35 π. In many applications error of 2% is acceptable in passband of low pass differentiator; therefore transition width can be optimized under this constraint. Salesnick's [24], Alaoui's [31] and Fourier Series approaches are compared with the convex optimization technique as in Figure 5.3 and Figure 5.4. It can be seen that designed differentiator's response is better in terms of transition region and sharp cut off characteristics. These features are important for suppression of high frequency noise.

5.2.3 Differentiator design with minimum *N*

In this case, available maximum order of the differentiator is provided and then an optimization procedure could be used to find minimum order filter. By solving the feasibility problems, filter length can be minimized. The feasibility check consists of same constraints as in (5.6), with passband ripple fixed. An optimization algorithm can be utilized to achieve minimum of n. For example, an efficient solution is bisection on n.

We can also pose the problem to design fractional order low pass differentiators as minmax formulation.

$$\begin{aligned} &\textit{minimize} \quad max \ \left|H\left(e^{j\omega}\right) - H_d(\omega)\right| && \omega \in [0, \omega_p] \\ &\textit{subject to} && H(\omega) \leq \delta && \omega \in [\omega_s, \pi] \end{aligned} \tag{5.7}$$

As an example, differentiator is designed with specifications design parameters taken are n = 37, v = 1.5, ω_p = 0.75 π, ω_s = 0.9 π. Magnitude response is plotted in Figure 5.3.

The same options that are discussed in the design of first order case can also be taken in fractional order differentiators.

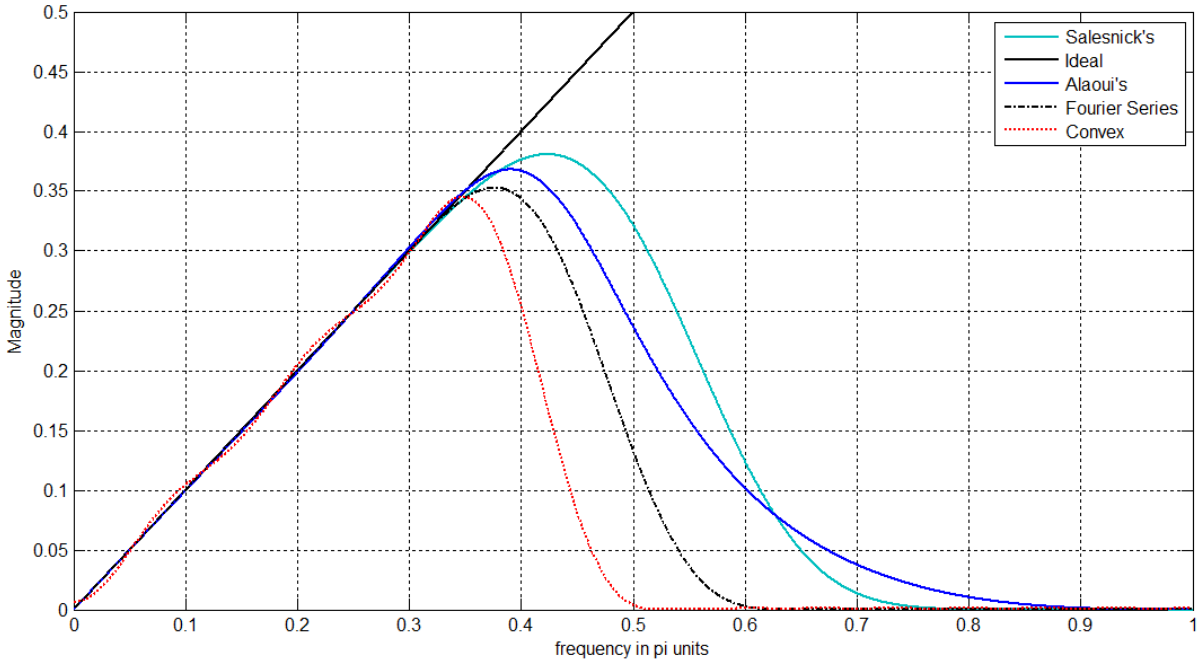

(a)

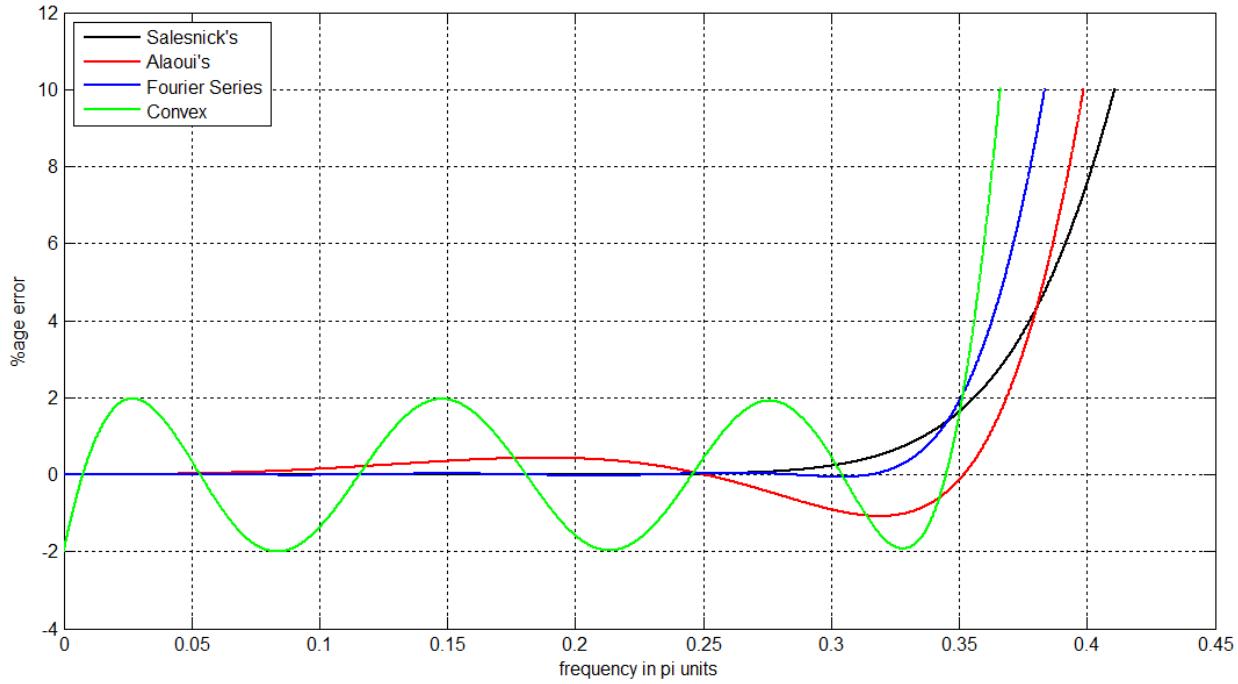

(b)

Figure 5.2: Low Pass Digital Differentiators with different design techniques (a) magnitude response (b) Error curves

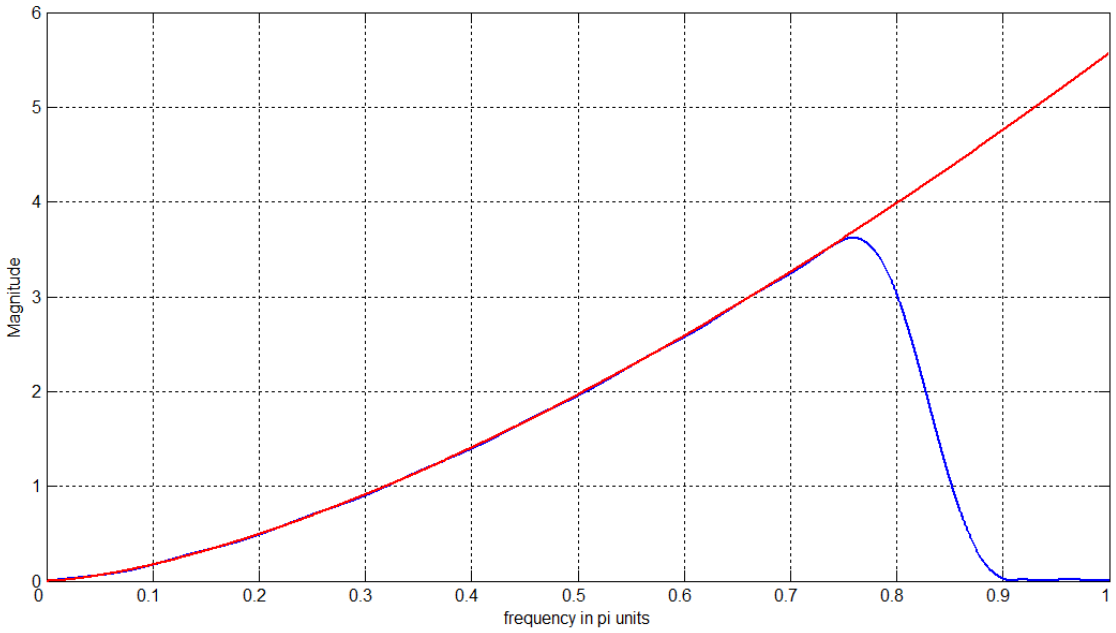

Figure. 5.3: Magnitude response of convex optimization based Low Pass FOD with order 1.5

5.3 Fractional Order Full Band Differentiator

In this section type IV fractional order digital differentiators are designed. To evaluate performance and compare different methods the integral squares error of frequency response is used

$$E = \frac{1}{\pi}\int_0^{\lambda\pi} \left|H\left(e^{j\omega}\right) - H_d(\omega)\right|^2 d\omega \tag{5.8}$$

To exploit above relation, minmax (Chebyshev) technique is applied on $\left|H\left(e^{j\omega}\right) - H_d(\omega)\right|$. Therefore the unconstrained convex optimization problem [13] can be stated as

$$\text{minimize} \quad max \underset{\omega\,\epsilon\,[0,\omega_p]}{sup} \left|H\left(e^{j\omega}\right) - H_d(\omega)\right| \tag{5.9}$$

In this example convex optimization approach is used to design a fractional order differentiator and it is compared with the frequency approximation method described in [23] as well as with Radial Basis Function (RBF) design technique [17]. It should be

noted that flexibility to change ω_p gives this approach an edge in terms of inband accuracy (α), this will be demonstrated in these design examples. Here design parameters taken are n = 10, v = 1.5, ω_p = 0.72 π, magnitude response is shown in Figure 5.5 (a). The parameters chosen in radial basis function method are n = 11, I = 5, v = 1.5, h = 0.05, L = 620 and Gaussian RBF with σ = 2.3, frequency response is illustrated in Figure 5.4 (a). The v equals 1.5 case of fractional order differentiator, designed in [23], is plotted in Figure 5.4(b).

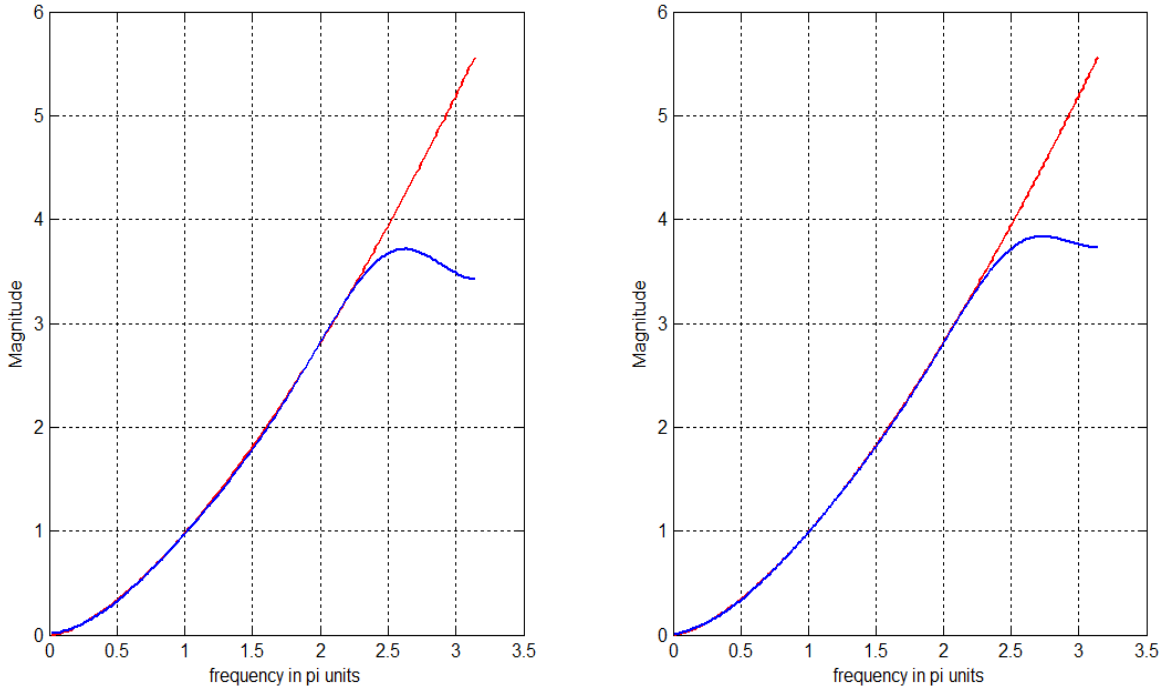

Figure 5.4: Magnitude response results of FODs using (a) Radial Basis Function (RBF) [17] (b) Frequency Response Approximation [23]

In [14], the differentiator was designed by minimizing error up to 0.72 π, however here we can easily minimize error with variable bandwidth. E for different values of λ of three of the methods is given in Table 5.2. Improvement in the optimization based FOD can be observed using $20log_{10}(E)$ parameter. It is evinced that convex optimization based method has improvement over RBF technique by 40.7 dB and 6.75 dB for λ=0.9 π and 0.72 π respectively, for the case of v = 1.5. Magnitude response of fractional differentiator for λ = 0.9 is shown in Figure 5.5(b). Hence frequency response is more easily and accurately approximated by convex optimization technique. It is observed that,

as ω_p is reduced in (5.9), the error (E) also decreases. It is because of the fact that the constraints imposed are less in reduced case.

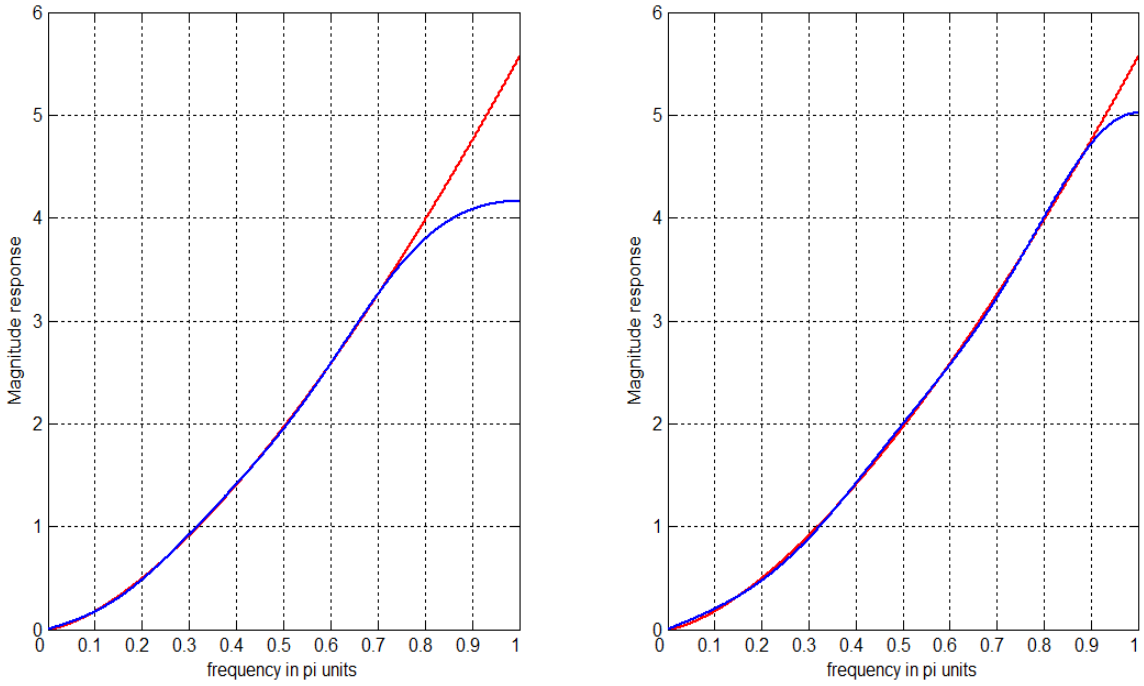

Figure 5.5: Magnitude response results of FODs using Convex Optimization (a) λ = 0.72 (b) λ = 0.9

Table 5.2: Integral squares error of convex optimization based FOD for $\lambda = 0.9\,\pi$, $0.72\,\pi$

	$E \quad for \quad \lambda = 0.9\,\pi$	$E \quad for \quad \lambda = 0.72\,\pi$
Convex	5.01 x 10^{-4}	8.13 x 10^{-5}
Radial Basis	0.0544	1.77 x 10^{-4}
Frequency Approximation	0.0358	1.77 x 10^{-5}

Another fractional order differentiator is designed with v = 0.5. The design specifications are n = 60, v = 0.5, $\omega_p = \pi$. In [17], authors have produced improved fractional order differentiator, using RBF, with respect to fractional delay method. In this design example same method is compared with RBF technique with specifications n = 61, I = 5, v = 0.5, h = 0.1, L = 620 and Gaussian RBF with σ = 2.3. E of RBF fractional order differentiator, for λ = 1, is 4.1 x 10^{-3} and error of convex optimization method is 6.04 x 10^{-5}. Therefore, 36.87 dB performance improvement is observed in convex optimization based FOD with respect to RBF based FOD. There are certain points to be taken care of such as slope of ideal differentiator's frequency response at $\omega = 0$ is infinity so some transition width should be provided at the point. Differentiator designed in [17] need modification in coefficients because of the non-zero gain at $\omega = 0$, however in this method there is no need of such modifications.

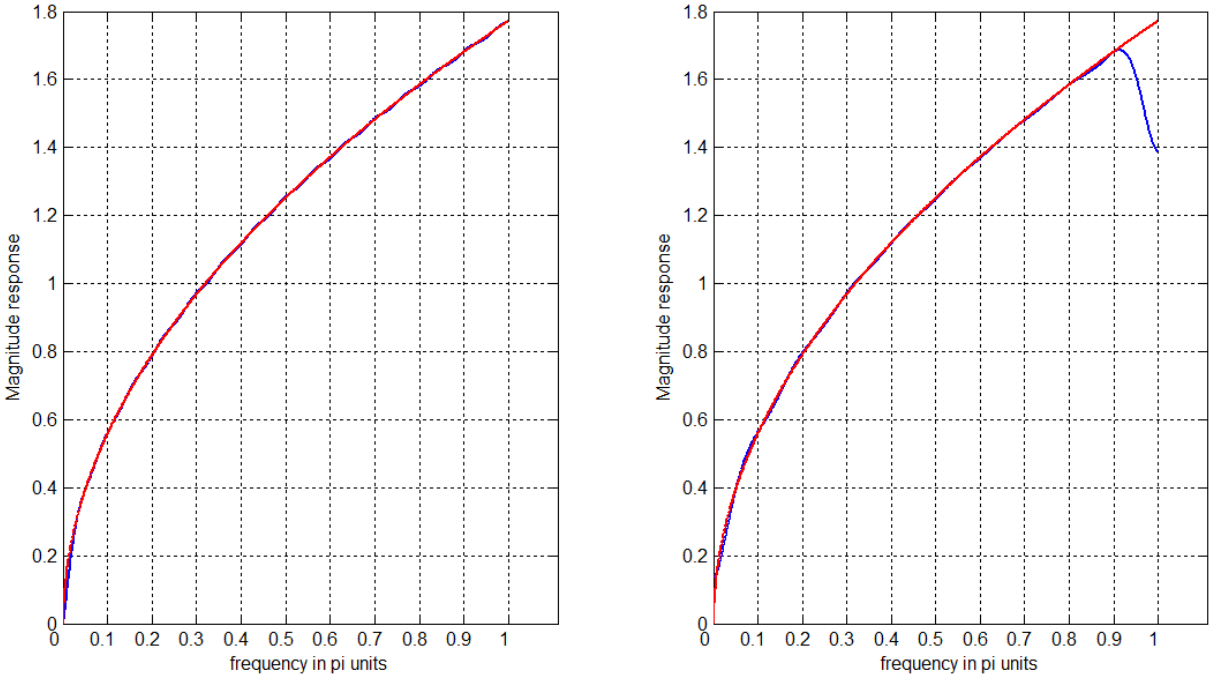

Figure 5.6: Magnitude response results of FODs for v = 0.5 using (a) Convex Optimization (b) Using RBF

Magnitude response of convex optimization based design is shown in Figure 5.6(a) and RBF based design in Figure 5.6(b). It is observed that optimization based design has better frequency approximation throughout the Nyquist interval as compared to RBF design.

5.4 IMAGE TEXTURE ENHANCEMENT

Image sharpening is a very useful image processing tool. It is used in many applications from medical imaging to artificial intelligence [17]. The purpose of sharpening is to highlight fine details in an image or to enhance details that have been blurred in image acquisition. In the literature, the sharpening is usually accomplished by spatial filters that based on second order derivative. Texture enhancement is needed due to blurring of the picture. Image sharpening is implemented in [17] by generalizing the concept of Laplacian method to fraction values. The same technique is used here to demonstrate the use of designed fractional order differentiator. The order of differentiation needed for same amount of image sharpening is relatively less in case of optimization based design as compared to RBF approach. The parameters for designed type IV differentiator are n = 6, $\omega_p = \pi$. The realization of implementation is shown in Figure 5.7. So that input image passes through the following two-dimensional (2-D) filter to get the sharpened image.

$$H(z_1, z_2) = 1 + B(z_1)B({z_1}^{-1}) + B(z_2)B({z_2}^{-1})$$

The larger order is, the stronger image sharpening is. This fact can be verified by using (51). So, users can select a suitable order to get a desired sharpened image. $f(x,y)$ is the original image and $p(x,y)$ is enhanced image. Some example images taken from [3] are demonstrated in Figure 5.8 to Figure 5.11. It can be observed that sharpening achieved here is at relatively lower order of differentiation than in RBF case [17].

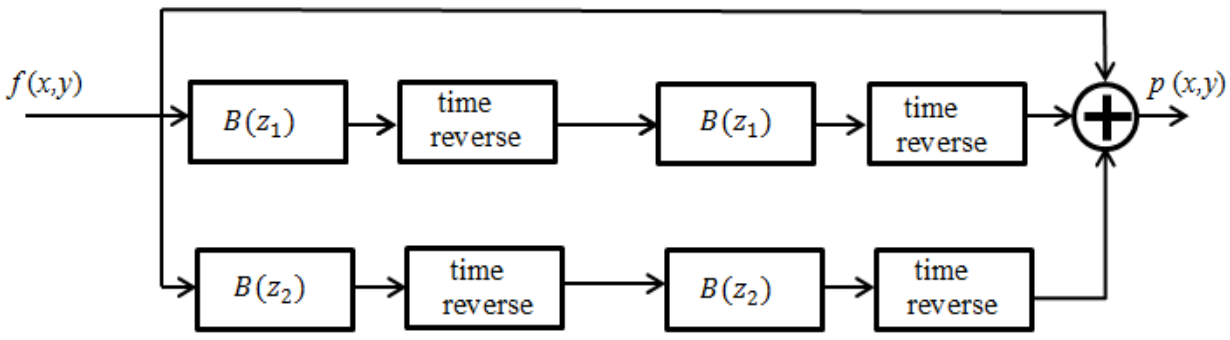

Figure 5.7: Realization method for image sharpening using fractional order differentiator [17]

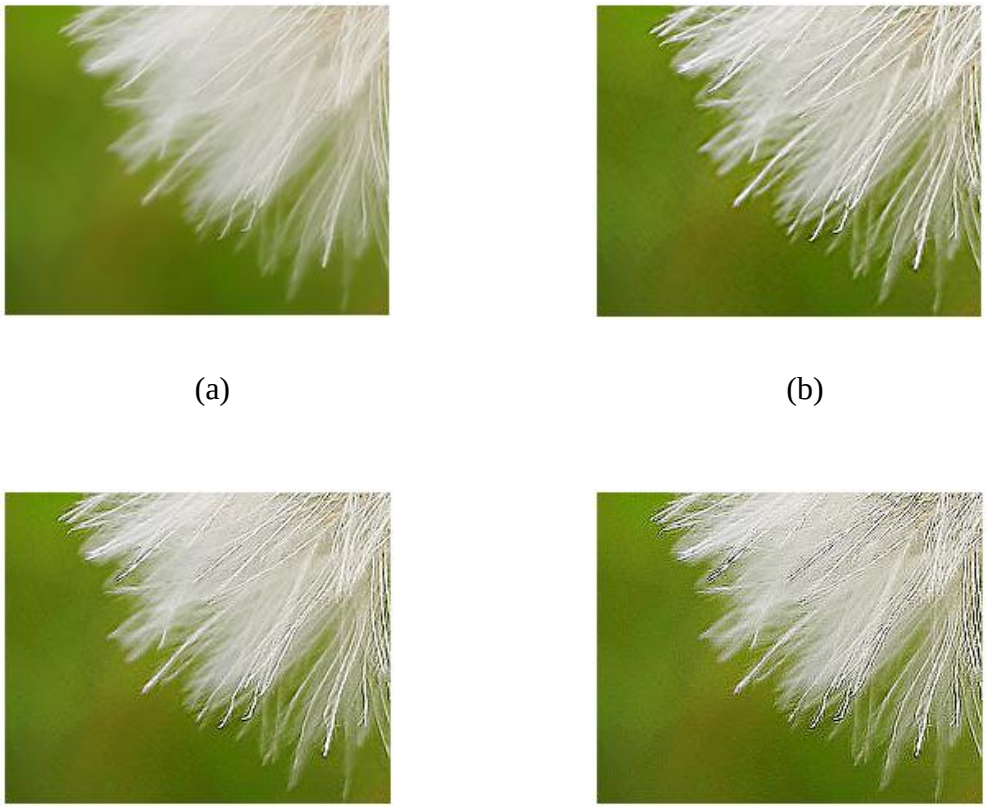

(a) (b)

(c) (d)

Figure 5.8: Dandelion image and enhanced images using various order of differentiation (a) Original image (b) v = 0.4 (c) v = 0.8 (d) v = 1.2

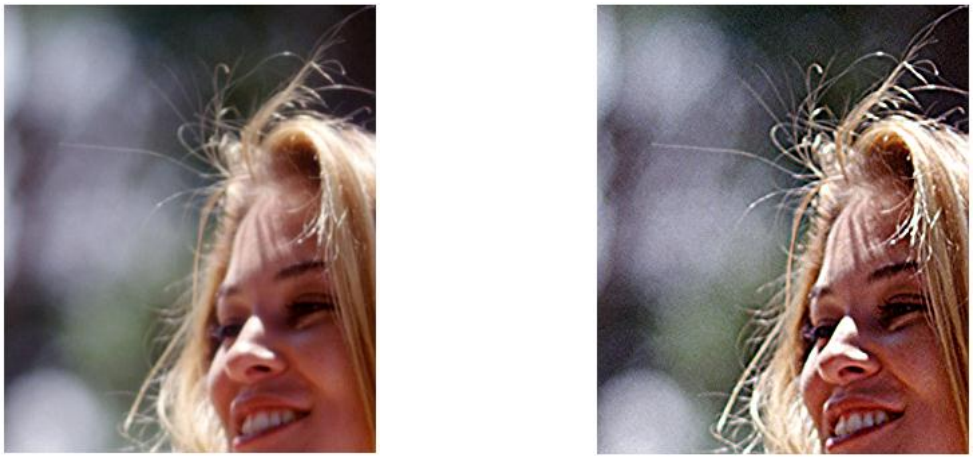

(a) (b)

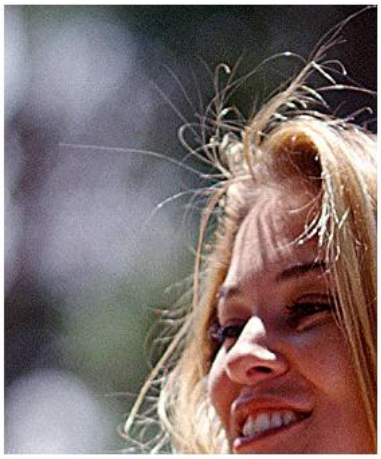

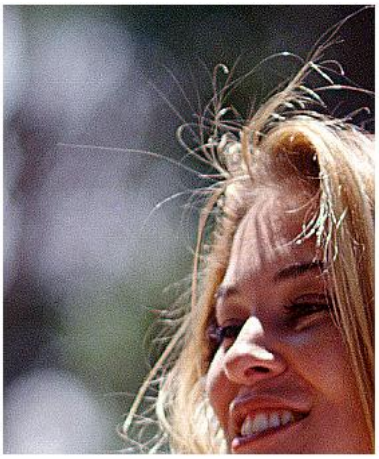

(c) (d)

Figure 5.9: Hair image and enhanced images using various order of differentiation. (a) Original image (b) v = 0.4 (c) v = 0.8 (d) v = 1.2

(a) (b)

(c) (d)

Figure 5.10: Toy image and enhanced images using various order of differentiation. (a) Original image (b) v = 0.4 (c) v = 0.8 (d) v = 1.2

(a) (b)

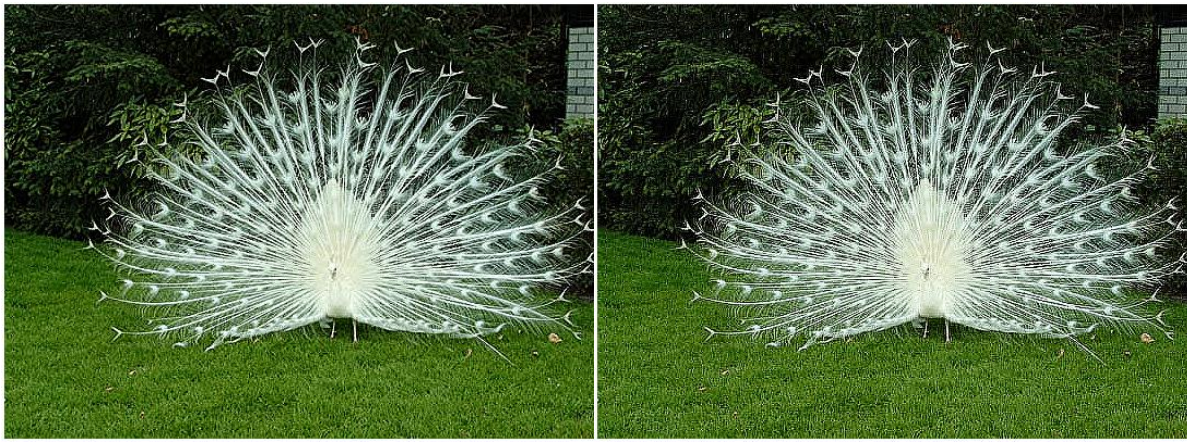

(c) (d)

Figure 5.11: Peacock image and enhanced images using various order of differentiation. (a) Original image (b) v = 0.4 (c) v = 0.8 (d) v = 1.2

5.5 Summary

The design of linear phase digital differentiators using convex optimization technique is investigated in this chapter. It is shown that various types of differentiator design problems can be formulated as convex semi-infinite problems. It is observed that the approach is very easy and gives us the flexibility to optimize desired parameter of the system. The method is then used to design first order low pass differentiators, we have discussed different options available separately. It is illustrated that the designed differentiator has less transition width and overshoot in frequency response, as compared to other techniques, [24] and [31]. The problem of fractional order case of low pass differentiator could also be solved by using minmax technique discussed in the paper. Fractional order differentiator designed employing the same method obtains better approximation in frequency response as compared to Radial Basis Function (RBF) [17] in terms of Mean Square Error (MSE). It is evinced that convex optimization based method has improvement over RBF technique by 40.7 dB and 6.75 dB for λ=0.9 π and 0.72 π respectively, for the case of v = 1.5. In case of v = 0.5, 36.87 dB performance improvement is observed in convex optimization based FOD with respect to RBF. An application of fractional order differentiator is shown as image texture enhancement. The

sharpening obtained by the differentiator is relatively greater than RBF method. So, convex optimization proves to be a very simple and effective tool for differentiator design according to application requirement. It would be interesting to extend the design methodology to two dimensional cases.

Chapter –6

Conclusion and Future Work

6.1 Conclusion

This thesis describes the design of higher and fractional order case of FIR digital differentiators. The length of impulse response of FIR differentiator is critical in many applications. Therefore, efficient use of number of coefficients is necessary. It can be achieved by improving frequency magnitude response available to us from current techniques.

First, this report describes the design of linear phase higher order case of FIR low pass digital differentiators. The formula to compute impulse response coefficients is derived using Fourier integral. This expression is used to design first order differentiator with variable normalized cutoff frequency using Kaiser Window. It provides an easy way to change cutoff frequency without altering the sampling frequency, reducing aliasing risk in the system. The frequency response of proposed differentiator is compared with Salesnick's [24] and Alaoui's [31] approaches. The proposed differentiator has relatively shorter transition regions and less overshoot in frequency response, resulting in suppression of high frequency noise. Flexibility in design process is observed due to possibility of window shaping parameter to fractions. Different design options available to user due to window shaping parameter are discussed separately. The options can also be taken in the case of second order differentiator. The formula is employed to obtain second order FIR low pass differentiator for QRS detection in ECG. The proposed algorithm enables us to detect R peaks even in presence of noise and baseline wanders, as demonstrated by processing MIT/BIH ECG recordings. It is also proved that the technique significantly reduces number of computations as compared to second derivative counterparts, which makes it suitable for real time processing of ECG waveform.

Then the design of linear phase digital differentiators using convex optimization technique is explored. It is shown that various types of differentiator design problems can be formulated as convex semi-infinite constrained and unconstrained problems. It is observed that the approach is very easy and gives us the flexibility to optimize desired

parameter of the system. The method is then used to design first order low pass differentiators, different options are discussed separately. It is illustrated that the proposed differentiator has even better frequency response, as compared to available methods. The problem of fractional order case of low pass differentiator is solved by using minmax technique. Full band FOD designed, using the same method, obtains superior approximation in frequency response as compared to Radial Basis Function (RBF) in terms of Mean Square Error (MSE). It is observed that the MSE of proposed convex optimization based method is better than RBF [17] technique's MSE by 40.7 dB and 6.75 dB for $\lambda = 0.9\,\pi$ and $0.72\,\pi$ respectively, for the case of v = 1.5. If order v = 0.5, then 36.87 dB performance improvement in MSE is observed in convex optimization based FOD with respect to RBF [17]. An application of fractional order differentiator is illustrated in the form of image texture enhancement. So, convex optimization proves to be a very simple and effective tool for differentiator design according to application requirement.

6.2 Future Research

Higher order low pass differentiators could well be used in applications like higher derivative based low frequency biomedical signal processing at a lower computational cost, finding applications, in different domains. It is interesting to seek other possible applications of the proposed filter design method in the future.

Generalization to include negative values of v to design differintegrators is also an area of further research. There is also chance to explore design of low pass integrators, differintegrators and extension to fractional order cases. It would be interesting to find applications which can benefit from these special types of filters.

Linear phase FIR FODs are designed using convex optimization in this thesis. By using constraints on magnitude response only we can design non-linear phase FODs. It could provide better results of magnitude response than linear phase counterparts.

References

[1] A. Antoniou, "Design of digital differentiators satisfying prescribed specifications", IEE Proceedings - E Computer Digital Techniques, vol. 127, pp. 24-30, Jan. 1980

[2] A. Antoniou and C. Charalambous, "Improved design method for Kaiser differentiators and comparison with equiripple method", ", IEE Proceedings - E Computer Digital Techniques, vol. 128, pp. 190-196, Sept. 1981

[3] A. Levin, D. Lischinski, Y. Weiss, "A closed-form solution to natural image matting", IEEE Trans. on Pattern Analysis and Machine Intelligence, vol. 30, pp. 228–242, Feb. 2008

[4] A. Ghaffari, H. Golbayani, M. Ghasemi, "A new mathematical based QRS detector using continuous wavelet transform", Computers and Electrical Engineering, vol. 34, pp. 81–91, 2008

[5] A. L. Goldberger et al., "PhysioBank, PhysioToolkit, and PhysioNet: Components of a new research resource for complex physiologic signals", Circulation, vol. 101, no. 3, pp. 215–220, 2000

[6] A.V. Oppenheim and R.W. Schafer, "Discrete-Time Signal Processing", Prentice-Hall, Englewood Cliffs, NJ, 1999.

[7] B. Datta, "Applied and Computational Control, Signals, and Circuits". In: S. P. Wu, S. Boyd, L. Vandenberghe, "FIR filter design via spectral factorization and convex optimization", Birkhauser, Cambridge, vol. 1, ch. 5, pp. 215–245, May 1999

[8] B. Kumar and S. C. Dutta Roy, “Coefficients of maximally linear FIR digital differentiators for low frequencies.” Electronic Letters, vol. 24, pp. 563-565, 1988

[9] B. Kumar, S. C. Dutta Roy, “On Digital Differentiators, Hilbert Transformers and Half Band low pass filters”, IEEE Trans. on education, vol. 32, no. 3, pp. 219–223, Aug. 1989

[10] B. Kumar, S. C. Dutta Roy and H. Shah, “On the design of FIR digital differentiators which are maximally linear at the frequency π/p, p = {positive integers}”, IEEE Trans. Acoustic Speech Signal Processing, vol. 40, pp. 2334-2338, 1992

[11] B. Carlsson, T. Soderstrom and A. Ahlen, “Digital differentiating filters”, Report UPTEC 8792R, Department of Technology, Uppsala University, Uppsala, Sweden, 1987

[12] C.C. Tseng, “Design of fractional order digital FIR differentiators”, IEEE Signal Process. Letters, vol. 8, pp. 77–79 , 2001

[13] C.C. Tseng, S.C. Pei and S.C. Hsia, “Computation of fractional derivatives using Fourier transform and digital FIR differentiator”, Signal Processing, vol. 80, pp. 151–159, 2000

[14] C. C. Tseng, “Series expansion design of variable fractional order integrator and differentiator using logarithm”, Signal Processing, vol. 88, no. 9, pp. 2278–2292, 2008.

[15] C.C. Tseng, “Design of variable and adaptive fractional order FIR differentiator”, Signal Processing, vol. 86, pp. 2554–2566, 2006

[16] C.C. Tseng, S.L. Lee, “Linear phase FIR differentiator design based on maximum signal-to-noise ratio criterion”, Signal Processing, vol. 86 , pp. 388-398, 2006

[17] C.C. Tseng and S.L. Lee, "Design of fractional order digital differentiator using radial basis function," IEEE Trans. on Circuits and Systems-I: Regular Papers, vol. 57, no. 7, pp. 1708-1718, Jul. 2010

[18] C. K. Chen and J. H. Lee, “Design of high-order digital differentiators using l_1, error criteria”, IEEE Trans. Circuits Syst. II: Analog Digit. Signal Process., vol. 42, no. 4, pp. 287-291, 1995

[19] E. C. Ifeachor and B. W. Jervis, “Digital Signal Processing”, 2nd ed. Englewood Cliffs, NJ, Prentice-Hall, 2002

[20] G.S. Mollova, R. Unbehauen, “Analytical design of higher order differentiators using least-squares technique”, Electron. Letters, vol. 37, pp. 1098–1099, 2001

[21] G. W. Medlin, “A design technique for high order digital differentiators”, International Conference on Acoustics, Speech and Signal Processing, pp. 1285 – 1288, vol.3, April 1990

[22] H. Hindi, “A Tutorial on Convex Optimization”, American Control Conference, Boston, pp. 3252-3265, 2004

[23] H. Zhao, G. Qiu, L. Yao, J. Yu, “Design of Fractional Order Digital FIR Differentiators using frequency response approximation”, Proceedings of the IEEE 2005 National Aerospace and Electronics Conference, vol.2, pp. 563-566, 2005

[24] I. Selesnick, “Maximally flat lowpass digital differentiators,” IEEE Trans. Circuits Syst. II, vol. 49, no. 3, pp. 219–223, Mar. 2002.

[25] J. F. Sturm, “Using SeDuMi 1.02, a Matlab toolbox for optimization over symmetric cones. Optim. Methods and Software”, vol. 11–12, pp. 625–653, 1999, [Online] Available: http://sedumi.ie.lehigh.edu

[26] J. G. Proakis and D. G. Manolakis, “Digital Signal Processing”. Englewood Cliffs, NJ: Prentice-Hall, 1996.

[27] K. B. Oldham and J.Spanier, “The Fractional Calculus”, Academic Press, New York, 1974.

[28] K. S. Miller and R. Ross, “An Introduction to the Fractional Calculus and Fractional Differential Equations”, New York, Wiley, 1993.

[29] L. R. Rabiner and B. Gold, “Theory and Application of Digital Signal Processing”, Prentice-Hall, Englewood Cliffs, NJ, 1975

[30] L. R. Rabiner and R. W. Schafer, “On the behavior of minimax relative error FIR digital differentiators”, Bell System Tech. Journal, vol. 53, pp. 331-361, 1974

[31] M. A. Al-Alaoui, “Linear phase low-pass IIR digital differentiators,” IEEE Trans. Signal Processing, vol. 55, no. 2, pp. 691–706, Feb. 2007.

[32] M. A. Al-Alaoui, "Novel approach to designing digital differentiators," IEEE Electronics Letters, vol. 28, no. 15, pp. 1376–1378, Jul. 1992.

[33] M. A. Al-Alaoui, "Novel digital integrator and differentiator," IEEE Electronics Letters, vol. 29, no. 4, pp. 376–378, Feb. 1993

[34] M. A. Al-Alaoui, "A class of second order integrators and lowpass differentiators," IEEE Trans. Circuits Syst. I, Fundamental Theory Applications, vol. 42, no. 4, pp. 220–223, Apr. 1995

[35] M. A. Al-Alaoui, "Direct approach to image edge detection using differentiators", International Conference on Electronics, Circuits and Systems 2010, pp. 154-157, 2009

[36] M. Grant, S. Boyd, "Graph implementations for nonsmooth convex programs. Recent Advances in Learning and Control", V. Blondel, S. Boyd, and H. Kimura, Eds. New York: Springer, pp. 95–110, 2008, [Online]. Available: http://stanford.edu/ ˜boyd/cvx

[37] N. Q. Ngo, "A New Approach for the Design of Wideband Digital Integrator and Differentiator", IEEE Trans. Circuits Syst. II: Express briefs, vol. 53, no. 9, pp. 936-940, Sept. 2006

[38] N.M. Arzeno, Z.D. Deng, C.S. Poon, "Analysis of first derivative based QRS detection algorithms", IEEE transactions on Biomedical Engineering, vol. 55, pp. 478-484, 2008

[39] G. E. Forsythe, M. A. Malcolm, C. B. Moler, "Computer Methods for Mathematical Computations", Prentice-Hall, 1976.

[40] G.M. Friesen, T.C. Jannett, M.A. Jadallah, S.L. Yates, S.R. Quint, H.T. Nagle, “A comparison of the noise sensitivity of nine QRS detection algorithms”, IEEE Trans. Biomedical Engineering, vol. 37, pp. 85–97, 1990

[41] P. Bois, “Table of Infinite Integrals”, Dover Publications, NY, 1962.

[42] P.B. Richard, “Algorithms for Minimization without Derivatives”, Prentice-Hall, Englewood Cliffs, New Jersey, 1973

[43] P.S. Hamilton, W.J. Tompkins, “Quantitative investigation of QRS detection rules using the MIT/BIH arrhythmia database”, IEEE Trans. Biomedical Engineering, vol. 33, pp. 1157–65, 1986

[44] R. J. Vanderbei, “Linear Programming: Foundations and Extensions”, Kluwer, Boston, 1996

[45] S. Boyd, L. Vandenberghe, “Convex Optimization”, Cambridge Univ. Press, Cambridge, U.K., 2004

[46] S.C. Pei, P.H. Wang and C.H. Lin, “Design of Fractional Delay Filter, Differintegrator, Fractional Hilbert Transformer, and Differentiator in Time Domain With Peano Kernel”, IEEE Trans. Signal Process., vol. 57, no. 2, pp. 391–403, Feb. 2010

[47] S.C. Pei, J.J. Shyu, “Eigenfilter design of higher-order digital differentiators”, IEEE Trans. Acoust. Speech Signal Processing, vol. 37, pp. 505–511,1989.

[48] S.C. Pei, J.J. Shyu, "Analytic closed form matrix for designing high order digital differentiators using eigen approach", IEEE Transactions Signal Processing, vol. 44, no. 3, pp. 698–701, 1996

[49] S.C. Dutta Roy, B. Kumar, "Digital differentiators" in: N.K. Bose, C.R. Rao, Handbook of Statistics, vol. 10, Elsevier Science Publishers, Amsterdam, pp.159-205, 1993

[50] S. K. Mitra, "Digital Signal Processing", Third edition, New York, McGraw-Hill, 2005

[51] S. Samadi, A. Omair, M.N.S. Swamy, "Exact fractional-order differentiators for polynomial signals", IEEE Signal Process. Letters, vol. 11, no. 6, pp. 529-532, June 2004

[52] T.N. Davidson, "Enriching the art of FIR filter design via Convex Optimization", IEEE Signal Processing Magazine, pp. 89-101, May 2010

[53] T. W. Parks and C. S. Burrus, "Digital Filter Design", John Wiley and Sons, 1987.

[54] V. Garg and K. Singh, "An Improved Grunwald-Letnikov Fractional Differential Mask for Image Texture Enhancement", International Journal of Advanced Computer Science and Applications, vol. 3, no. 3, pp. 130-135, 2012

[55] Y. Q. Chen and B. M. Vinagre, "A new IIR-type digital fractional order differentiator," Signal Processing, vol. 83, no. 11, pp. 2359–2365, Nov. 2003.